

Clark University

Clark Digital Commons

Student Publications

Student Works

3-6-2023

Evaluation of Risk of Bias in Neuroimaging-Based Artificial Intelligence Models for Psychiatric Diagnosis: A Systematic Review

Zhiyi Chen

Xuerong Liu

Qingwu Yang

Yan-Jiang Wang

Kuan Miao

See next page for additional authors

Follow this and additional works at: https://commons.clarku.edu/student_publications

 Part of the Psychology Commons

Authors

Zhiyi Chen, Xuerong Liu, Qingwu Yang, Yan-Jiang Wang, Kuan Miao, Zheng Gong, Yang Yu, Artemiy Leonov, Chunlei Liu, Zhengzhi Feng, and Hu Chuan-Peng



Original Investigation | Health Informatics

Evaluation of Risk of Bias in Neuroimaging-Based Artificial Intelligence Models for Psychiatric Diagnosis

A Systematic Review

Zhiyi Chen, PhD; Xuerong Liu, MS; Qingwu Yang, MD; Yan-Jiang Wang, MD; Kuan Miao, MS; Zheng Gong, MS; Yang Yu, MPH; Artemiy Leonov, MPH; Chunlei Liu, PhD; Zhengzhi Feng, PhD, MD; Hu Chuan-Peng, PhD

Abstract

IMPORTANCE Neuroimaging-based artificial intelligence (AI) diagnostic models have proliferated in psychiatry. However, their clinical applicability and reporting quality (ie, feasibility) for clinical practice have not been systematically evaluated.

OBJECTIVE To systematically assess the risk of bias (ROB) and reporting quality of neuroimaging-based AI models for psychiatric diagnosis.

EVIDENCE REVIEW PubMed was searched for peer-reviewed, full-length articles published between January 1, 1990, and March 16, 2022. Studies aimed at developing or validating neuroimaging-based AI models for clinical diagnosis of psychiatric disorders were included. Reference lists were further searched for suitable original studies. Data extraction followed the CHARMS (Checklist for Critical Appraisal and Data Extraction for Systematic Reviews of Prediction Modeling Studies) and PRISMA (Preferred Reporting Items for Systematic Reviews and Meta-analyses) guidelines. A closed-loop cross-sequential design was used for quality control. The PROBAST (Prediction Model Risk of Bias Assessment Tool) and modified CLEAR (Checklist for Evaluation of Image-Based Artificial Intelligence Reports) benchmarks were used to systematically evaluate ROB and reporting quality.

FINDINGS A total of 517 studies presenting 555 AI models were included and evaluated. Of these models, 461 (83.1%; 95% CI, 80.0%-86.2%) were rated as having a high overall ROB based on the PROBAST. The ROB was particularly high in the analysis domain, including inadequate sample size (398 of 555 models [71.7%; 95% CI, 68.0%-75.6%]), poor model performance examination (with 100% of models lacking calibration examination), and lack of handling data complexity (550 of 555 models [99.1%; 95% CI, 98.3%-99.9%]). None of the AI models was perceived to be applicable to clinical practices. Overall reporting completeness (ie, number of reported items/number of total items) for the AI models was 61.2% (95% CI, 60.6%-61.8%), and the completeness was poorest for the technical assessment domain with 39.9% (95% CI, 38.8%-41.1%).

CONCLUSIONS AND RELEVANCE This systematic review found that the clinical applicability and feasibility of neuroimaging-based AI models for psychiatric diagnosis were challenged by a high ROB and poor reporting quality. Particularly in the analysis domain, ROB in AI diagnostic models should be addressed before clinical application.

JAMA Network Open. 2023;6(3):e231671. doi:10.1001/jamanetworkopen.2023.1671

Key Points

Question Are there potential risks to translating neuroimaging-based artificial intelligence (AI) models into direct clinical applications, such as psychiatric diagnosis?

Findings In this systematic review of 517 studies presenting 555 neuroimaging-based AI models for psychiatric diagnostics, most models had a high overall risk of bias and had poor clinical applicability. All articles provided incomplete reports for validation.

Meaning Findings of this study suggest that, in their current form, neuroimaging-based AI models for psychiatric diagnosis need to address risk of bias before use in clinical practice.

+ Supplemental content

Author affiliations and article information are listed at the end of this article.

Open Access. This is an open access article distributed under the terms of the CC-BY-NC-ND License.

Introduction

Given the lack of biomarkers to guide psychiatric diagnoses, machine learning has been increasingly applied to develop brain-based hallmarks. Thus, neuroimaging-based artificial intelligence (AI) models have proliferated rapidly during the past 3 decades. Rather than enabling a clinician-based diagnosis of discrete symptoms, neuroimaging-based AI models enable an objective, symptom-centered, individualized and neurobiologically explicable estimate of psychiatric conditions.^{1,2} In this vein, these models show considerable potential to be translated for use in early diagnosis, treatment development, and clinical decision-making.³⁻⁷ However, lack of an evidence-based systematic appraisal of AI models impedes stakeholder enthusiasm for applying them in clinical practice.^{8,9}

Systematic appraisals of clinical AI models may provide solid evidence to validate their reliability in medical practice. For instance, despite global efforts to develop AI diagnostic models for COVID-19, these models built either through traditional multivariable analysis or imaging-based AI technique were found to have poor clinical implications due to a high risk of bias (ROB).^{10,11} Furthermore, systematic appraisals revealed the high ROB in clinical models across all medical specialties, especially in psychiatric diagnoses.^{12,13} During the past 3 decades, advances in neuroimaging-based techniques opened radically new venues for psychiatric diagnosis by providing potentially more reliable and sensitive brain biomarkers in AI prediction models.^{14,15} Despite their strengths, the absence of systematic appraisals for biomarker-based AI models leaves a gap between the experimental proof-of-concept models and clinical applicability.

In addition, poor reporting quality impedes the establishment of better practices in AI-based psychiatric diagnosis. Despite the developments of multifarious benchmarks for reporting clinical prediction models (eg, STARD [Standards for Reporting of Diagnostic Accuracy], DECIDE-AI [Early-Stage Clinical Evaluation of Decision Support Systems Driven by Artificial Intelligence], and TRIPOD [Transparent Reporting of a Multivariable Prediction Model for Individual Prognosis or Diagnosis]),¹⁶⁻¹⁹ the reporting quality in current publications still needs to be improved, with approximately 80% of articles providing incomplete information and less than 50% of contents following the TRIPOD guideline, limiting clinical potential and contributing to research waste.²⁰⁻²² Even after 3 decades of neuroimaging-based AI model developments, it remains unclear whether the reports of such developments are unbiased and complete enough to warrant translation into clinical practice for psychiatric diagnosis.

In this study, we sought to systematically assess the ROB and reporting quality of neuroimaging-based AI models for psychiatric diagnosis that were developed in the past 3 decades. To this end, we used the Prediction Model Risk of Bias Assessment Tool (PROBAST) and modified Checklist for Evaluation of Image-Based Artificial Intelligence Reports (CLEAR) benchmarks.^{23,24}

Methods

The study protocol was registered at PROSPERO ([CRD42022340624](https://doi.org/10.1186/1745-2974-4-624)) and followed the Preferred Reporting Items for Systematic Reviews and Meta-analyses (PRISMA) reporting guideline (Figure 1²⁵⁻⁵⁴¹).^{542,543} The Chinese Army Medical University Institutional Review Board officially censored the study and deemed it exempt from approval and the requirement for informed consent given that no original human or animal participants were involved.

Retrieval Strategy

Following retrieval benchmarks,^{543,544} we conducted a literature search in PubMed in June 2022 using Boolean codes and RSS (Really Simple Syndication) feeds (eMethods 1 in Supplement 1). We initially included studies that (1) were published between January 1, 1990, and March 16, 2022; (2) were peer-reviewed, full-length original articles published in journals or conference proceedings; and (3) developed or validated neuroimaging-based AI models for diagnosing psychiatric diseases that were defined in the *Diagnostic and Statistical Manual of Mental Disorders* (Fifth Edition).

We screened studies from the initial literature pool by following these inclusion criteria: (1) at least 1 algorithm was used to build the AI model for psychiatric diagnosis; (2) training features were limited to neuroimaging-based biomarkers (eg, [functional] magnetic resonance imaging, electroencephalogram, and functional near-infrared spectroscopy); and (3) minimum fundamental information for the AI model was reported. Reference lists were further searched for suitable original studies. Exclusion criteria were articles that (1) were not peer-reviewed original research (eg, preprint, review, meta-analysis, or comments), (2) involved non-neuroimaging-based features (eg, behavioral factors or blood and genes) or nonhuman participants, (3) used nondiagnostic AI models (eg, prognostic model) for unclassified psychiatric disorders, and (4) used discriminatory AI algorithm that differentiated cohorts rather than diagnosed psychiatric conditions.

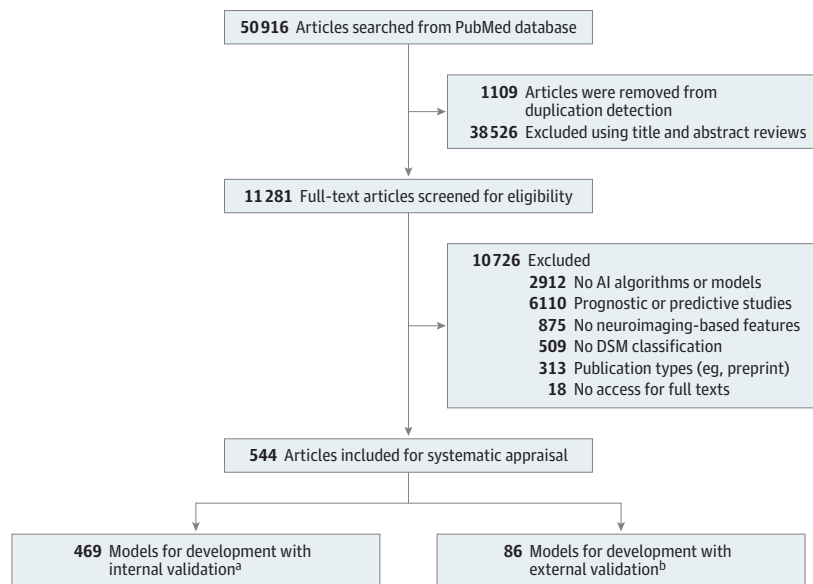
Data Extraction and Analysis

Data extraction adhered to the CHARMS (Checklist for Critical Appraisal and Data Extraction for Systematic Reviews of Prediction Modeling Studies) and PRISMA guidelines.^{19,544} We used a closed-loop cross-sequential design for quality control on data extraction and screening (5 assessors). Details on data extraction are provided in eMethods 2 and 3 in Supplement 1.

We built on a global geospatial model to illustrate the distribution of the sample population for these AI models. Sample population was defined according to information in the original article if applicable (eMethods 3 in Supplement 1). Global geospatial map was constructed by first fine-grained classification, which included 251 countries or regions. Geospatial source data were adjusted by the United Nations Statistics Division M49 codes and EasyShu team.

The PROBAST²⁴ was used to assess the ROB of the neuroimaging-based AI models for psychiatric diagnosis. The PROBAST encompassed 20 signaling questions covering 4 ROB domains: participants, predictors, outcome, and analysis. Each question may be answered by yes, probably yes, no, probably no, or no information. Answering *no* or *probably no* to a signaling question indicated a potential high ROB. Overall ROB was rated high if a *no* or *probably no* answer was given for any signaling question. Overall low ROB was defined as answering all of the signaling questions with a *yes* or *probably yes*. The PROBAST criterion was modified to assess its applicability to each included

Figure 1. Evidence Review Pipeline Based on PRISMA 2020 Guideline



DSM indicates *Diagnostic and Statistical Manual of Mental Disorders*.

^a Of the 555 artificial intelligence (AI) models, 469 were tested at the internal sample and 86 at the independent external sample, including intellectual disability,²⁵⁻²⁸ autism spectrum disorder,²⁹⁻¹⁴⁷ attention-deficit/hyperactivity disorder,^{44,51,72,148-381} bipolar disorder,^{290,314,321,327,328,339,343,346,382-406} major depressive disorder,^{309,346,359,363,381,405,407-473} social anxiety disorder,⁴⁷⁴⁻⁴⁷⁷ unspecified anxiety disorder,^{346,478,479} general anxiety disorder,⁴⁸⁰ obsessive-compulsive disorders,^{346,481-496} posttraumatic stress disorder,^{346,409,497-503} somatic symptom disorder,⁵⁰⁴ anorexia nervosa,⁵⁰⁵⁻⁵⁰⁷ binge-eating disorder,⁵⁰⁸ insomnia disorder,^{509,510} conduct disorder,⁵¹¹⁻⁵¹³ antisocial personality disorder,⁵¹⁴⁻⁵¹⁶ other or unknown substance use disorder,⁵¹⁷⁻⁵²⁰ alcohol use disorder,^{346,521-536} opioid use disorder,⁵³⁷ borderline personality disorder,⁵³⁸⁻⁵⁴⁰ disruptive behavior disorders,⁵⁴¹ and social anxiety disorder.³⁴⁶

^b Eighty-six AI models^{30,32,34,36,42,44,46,53,59-61,63,69,70,72,81,82,88,91,117,149,151,156,162-164,169,170,172,180,182,187,191,197,212,213,220,221,247,254,258,260,261,263,269,272,278,280,283-285,287,290,301,305,307,319,335,352,353,355,356,359,385,407,417,422,443,452,454,483,484,510,519,526,532,534} were tested at the independently external sample.

study by adding 1 signaling question for the first 3 ROB domains (participants, predictors, and outcome) (eMethods 4 in [Supplement 1](#))

We adopted the modified 25-item CLEAR statement²³ to evaluate the reporting quality (ie, feasibility) of the included studies, which included 4 domains (data, technique, technical assessment, and applications). To ensure applicability to neuroimage-based AI models, we removed 3 items (eMethods 5 in [Supplement 1](#)). The eligible 22 items were transformed for signaling questions to form the modified CLEAR statement (eTable 1 in [Supplement 1](#)). The CLEAR criteria for assessing the overall reporting quality of these studies were fully in line with the PROBAST.

To ensure adequate assessment validity, 5 independent assessors with multidisciplinary expertise were involved, including a clinical psychiatrist (Y.Y.), research fellows for psychiatry (X.L.) and AI (K.M.), a neuroscientist (Z.G.), and a psychologist (Z.C.). We built a closed-loop cross-sequential framework for validating assessment quality. Furthermore, another independent assessor (C.L.) was invited to validate assessment quality (eMethods 6 in [Supplement 1](#)).

Statistical Analysis

Geospatial models were built using R packages, version 4.0.5 (R Core Team). Interactive interfaces for sample population map were generated from EasyShu, version 2.4 (EasyShu) and coded with C++. Bootstrapping simulation (n = 2000) was performed to estimate 95% CIs for proportions using MATLAB (MathWorks Inc). Cohen κ test was also conducted to quantify the reliability of assessment quality across these 5 subsets. A prior 2-sided significance level for these statistics was set as $P = .05$.

Results

A total of 517 studies presenting 555 development-purpose AI models were eligible for inclusion in the analysis²⁵⁻⁵⁴¹ from the 50 916 records that were retrieved from the PubMed search in June 2022. Of the 555 models, 469 (84.5%) were for internal-sample validation^{25-29, 31, 33, 35, 37-41, 43, 45, 47-52, 54-58, 62, 64-68, 71, 73-80, 83-87, 89, 90, 92-116, 118-127, 129-134, 136, 139-145, 147, 148, 150, 152-155, 157-161, 165-168, 171, 173-179, 181, 183-186, 188-196, 198-211, 214-219, 222-246, 248-253, 255-257, 259, 262, 264-268, 270, 271, 273-277, 279, 281, 282, 286, 288, 289, 291-300, 302-304, 306, 308-318, 320-334, 336-351, 354, 357, 358, 360-384, 386-406, 408-416, 418-442, 444-451, 453, 455-469, 471-482, 485-502, 504-509, 511-518, 520-525, 527-531, 533, 535-541} and 86 (15.5%) were for external-sample validation^{30, 32, 34, 36, 42, 44, 46, 53, 59-61, 63, 69, 70, 72, 81, 82, 88, 91, 117, 128, 135, 137, 138, 146, 149, 151, 156, 162-164, 169, 170, 172, 180, 182, 187, 197, 212, 213, 220, 221, 247, 254, 258, 260, 261, 263, 269, 272, 278, 280, 283-285, 287, 290, 301, 305, 307, 319, 335, 352, 353, 355, 356, 359, 385, 407, 417, 422, 443, 452, 454, 470, 483, 484, 503, 510, 519, 526, 532, 534} (Figure 1). Based on the United Nations Statistics Division classification, the samples for training or testing these models covered 15.5% (39 of 251) of countries or areas globally (Figure 2), with 97.5% (38 of 39) of samples located in high-income or upper-middle-income areas.

Nearly half of the models (48.3% [268 of 555]) were found in studies authored by those with academic training in computers and data science^{27, 32-37, 39-42, 44-48, 50, 52, 58, 70-73, 75, 76, 79, 82, 85, 87, 89, 90, 92, 93, 95, 96, 99-118, 121, 123, 128-130, 132-136, 139, 141, 142, 144, 146, 151, 152, 156, 161-164, 166-168, 170, 173, 175-177, 179, 180, 182, 184, 185, 187, 190, 193, 195, 200, 202, 204-206, 208-210, 212, 214, 220, 224-228, 230, 232-235, 239, 240, 245, 247, 250, 251, 256, 257, 259, 260, 263, 266, 271, 272, 275-277, 283, 288, 289, 293, 297, 301-303, 306, 308, 311, 313, 314, 316, 318-320, 323-326, 328-336, 339-341, 344, 345, 348, 350, 353, 354, 357-359, 362, 365-380, 392, 394, 399, 401-403, 410, 411, 413-416, 425, 430-433, 436, 440, 445-449, 451, 452, 455-457, 462, 463, 465, 466, 469, 470, 472, 476, 478-480, 484, 488-491, 496, 510-513, 516, 519, 520, 523, 525, 526, 530, 531, 533-535, 537, 539, 541} (eTable 2 in [Supplement 1](#)). Schizophrenia (25.4% [141 of 555 models])²⁴⁷⁻³⁸¹ and autism spectrum disorder (21.4% [119 of 555 models])²⁹⁻¹⁴⁷ were the most common psychiatric diseases to be diagnosed with these models (eTable 3 in [Supplement 1](#)). Full technical details are provided in eTables 3 to 9 in [Supplement 1](#). Assessor reliability quality was found to be satisfied, with an acceptable Cohen κ coefficient mean of 0.68 (median [range], 0.96 [0.02-1.00]) across 5 subset pools (eMethods 6 in [Supplement 1](#)).

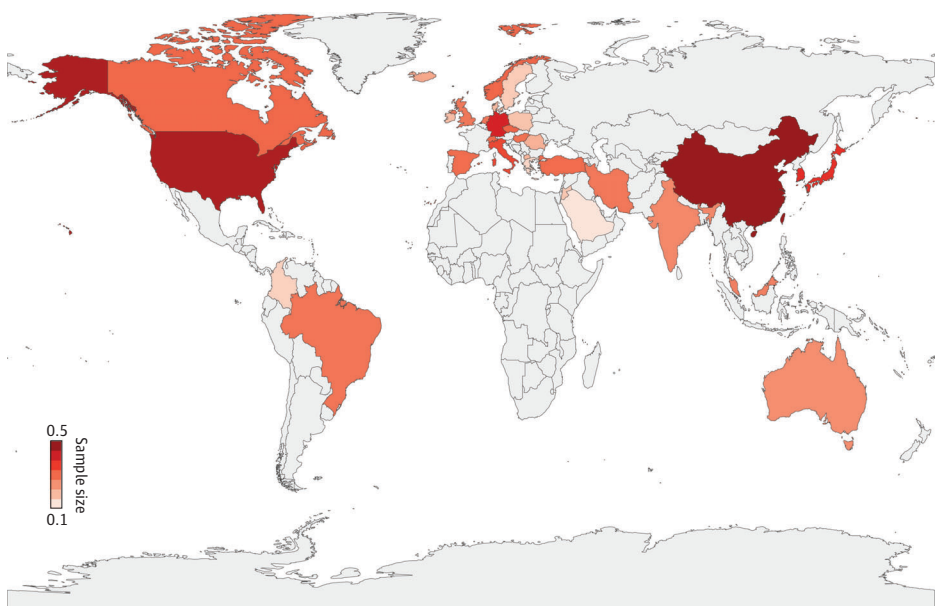
Overall ROB for AI Models

In total, 461 of 555 AI models (83.1%; 95% CI, 80.0%-86.2%) were rated as having high overall ROB.^{25, 32-41, 43-50, 52-60, 62-69, 71-81, 83, 85, 87-92, 94-111, 113-124, 126-130, 133, 135, 136, 141, 142, 145, 146, 148, 149, 151, 153, 155, 156, 158, 161, 163, 166-170, 172-177, 179-183, 186, 187, 189-193, 195, 197-212, 214-227, 229, 230, 232-242, 245-247, 249, 251-253, 256-260, 262, 264, 265, 268, 270, 273-281, 283-322, 324-336, 338-345, 347-370, 372-426, 428-435, 439-462, 464-473, 475, 477-480, 482-485, 487, 491, 493, 495, 498, 500, 502-505, 507-513, 515-517, 519-533, 536-541} Two of 555 models (0.4%; 95% CI, 0.00%-0.01%) were rated with high overall ROB in the participants domain.^{26,31} Overall, the ROB in the participants domain remained low for existing neuroimaging-based AI diagnostic models.

In the predictors domain, 187 of 555 models (33.7%; 95% CI, 29.9%- 37.6%) were rated with high ROB^{37, 38, 47, 55-57, 59, 60, 62, 68, 69, 78, 79, 81, 85, 89, 92, 99, 100, 104, 107, 113, 115, 117, 121, 129, 130, 133, 135, 136, 148, 150, 154, 158, 160, 161, 167, 169, 170, 173, 175, 178, 183, 190, 191, 193, 195, 197, 201, 204, 206, 207, 210, 212, 215, 216, 224, 225, 229, 232-235, 238, 240, 242, 247, 251, 253, 257, 260, 274, 277, 279, 283, 285, 286, 290, 295, 299, 303-307, 317-320, 322, 326, 332-336, 339, 340, 345, 347, 349-353, 357, 358, 360, 363-365, 376, 385, 388-393, 398, 400, 402-406, 409-411, 413, 415-418, 421, 423-426, 428-430, 433, 434, 441, 442, 444, 449, 451, 452, 459, 461, 464, 466, 468, 472, 475, 478, 484, 488, 491, 493, 502, 504, 505, 516, 529, 532, 533, 537, 538, 540, 541} (Table 1). Defining predictors by knowing the outcome of these models was the unique source of the high ROB in this domain (ie, signaling question 2.2: were predictor assessments made without knowledge of outcome data?). In the outcome domain, high ROB was scored for 198 of 469 models (35.7%; 95% CI, 31.8%-39.7%)^{26, 32, 33, 35-37, 39, 41, 44, 45, 48, 53-57, 59, 60, 62, 68, 69, 78, 79, 81, 85, 89, 92, 99, 100, 104, 107, 113, 115, 117, 121, 129, 130, 133, 135, 136, 148, 150, 154, 158, 160, 161, 167, 169, 170, 173, 175, 178, 183, 190, 191, 193, 195, 197, 201, 204, 206, 207, 210, 212, 215, 216, 224, 225, 229, 232-235, 238, 240, 242, 247, 251, 253, 257, 260, 274, 277, 279, 283, 285, 286, 290, 295, 299, 303-307, 317-320, 322, 326, 332-336, 339, 340, 345, 347, 349-353, 357-360, 363-365, 376, 385, 388-393, 398, 400, 402-406, 409-411, 413, 415-418, 421, 423-426, 428-430, 433, 434, 441, 442, 444, 449, 451, 452, 459, 461, 464, 466, 468, 472, 475, 478, 484, 488, 491, 493, 502, 504, 505, 516, 529, 532, 533, 537, 538, 540, 541} (Table 1). These models had a high ROB because the outcome knowledge of testing data sets was leaked into the predictors of the training set (ie, signaling question 3.3: were predictors excluded from the outcome definition?).

In the analysis domain, most models were rated as having high overall ROB (461 of 555 [83.1%; 95% CI, 80.0%-86.2%]).^{25, 32-41, 43-50, 52-60, 62-69, 71-81, 83, 85, 87-92, 94-111, 113-124, 126-130, 133, 135, 136, 141, 142, 145, 146, 148, 149, 151, 153, 155, 156, 158, 161, 163, 166-170, 172-177, 179-183, 186, 187, 189-193, 195, 197-212, 214-227, 229, 230, 232-242, 245-247, 249, 251-253, 256-260, 262, 264, 265, 268, 270, 273-281, 283-322, 324-336, 338-345, 347-370, 372-421, 423-426, 428-435, 439-462, 464-473, 475, 477-480, 482-485, 487, 491, 493, 495, 498, 500, 502-505, 507-513, 515-517, 519-533, 536-541} Inadequate

Figure 2. Geospatial Model for Sample Population



Total sample sizes for countries were geologically mapped into corresponding location in the global map. To improve readability, original total sample size underwent log-transformation.

sample size (398 of 555 [71.7%; 95% CI, 68.0%-75.6%]),^{25-31, 33, 35, 37-41, 43, 45, 46, 48, 49, 54-61, 64-67, 70, 71, 73, 77, 79, 80, 82-85, 87-92, 94-101, 106, 108, 110, 111, 113, 114, 119, 120, 122, 124, 126, 128, 129, 133-135, 137, 138, 141-144, 146-149, 151-153, 155, 156, 161, 163, 164, 166, 169, 171, 172, 174, 175, 177-180, 182, 183, 185-191, 194, 195, 197, 199, 203-205, 207, 209-212, 214-220, 222-227, 229, 230, 232, 233, 236, 237, 239-243, 246, 247, 249, 250, 252, 256-267, 269, 270, 274, 277-279, 281-283, 285-297, 300-304, 307, 309-311, 313-316, 320-325, 328-336, 338, 340-345, 347-356, 358, 359, 361, 364, 366, 369-390, 392, 393, 396-401, 403-417, 419-421, 423-445, 447-452, 454, 456, 459-462, 464-469, 472, 473, 477, 480, 482-484, 487-490, 492-496, 498, 501-504, 507, 508, 512, 513, 515-517, 519-532, 536-540} poor model performance examination (with 100% of models lacking calibration examination), and lack of handling data complexities (550 of 555 [99.1%; 95% CI, 98.3%-99.9%]),^{27,28,31-541} with the majority of models undergoing no adjustment on data complexities [eg, signal question 4.6: were complexities in the data, such as censoring, competing risks, and sampling of control participants, accounted for appropriately?] all contributed to the potential high ROB of these AI models in the analysis domain (Table 1). Although almost all of the models were rated with high ROB on calibration and data complexities issues, 52 models^{27,28, 31, 42, 51, 61, 70, 82, 84, 86, 93, 112, 132, 139, 171, 184, 213, 228, 231, 243, 244, 248, 250, 254, 255, 261, 263, 266, 269, 271, 272, 282, 323, 337, 346, 371, 422, 436-438, 463, 474, 476, 481, 486, 506, 514, 518, 534, 535} were still rated with low overall ROB in the analysis domain because these issues were judged as having limited implications for the models.

Table 1. ROB Assessment for All Included AI Models Using the PROBAST (N = 555)

Signaling question ^a	Answers, No. (%)		
	Yes or probably yes	No information	No or probably no
Domain 1: participants			
Were appropriate data sources used (eg, cohort, RCT, or nested case-control study data)?	555 (100.0)	0	0
Were all inclusions and exclusions of participants appropriate?	553 (99.6)	0	2 (0.4)
Domain 2: predictors			
Were predictors defined and assessed in a similar way for all participants?	555 (100.0)	0	0
Were predictor assessments made without knowledge of outcome data?	368 (66.3)	0	187 (33.7)
Were all predictors available at the time the model was intended to be used?	555 (100.0)	0	0
Domain 3: outcome			
Was the outcome determined appropriately?	555 (100.0)	0	0
Was a prespecified or standard outcome definition used?	555 (100.0)	0	0
Were predictors excluded from the outcome definition?	357 (64.3)	0	198 (35.7)
Was the outcome defined and determined in a similar way for all participants?	555 (100.0)	0	0
Was the outcome determined without knowledge of predictor information?	358 (64.5)	0	197 (35.5)
Was the time interval between predictor assessment and outcome determination appropriate?	555 (100.0)	0	0
Domain 4: analysis			
Was there a reasonable number of participants with the outcome?	157 (28.2)	0	398 (71.7)
Were continuous and categorical predictors handled appropriately?	555 (100.0)	0	0
Were all enrolled participants included in the analysis?	393 (70.9)	0	162 (29.1)
Were participants with missing data handled appropriately?	44 (7.9)	37 (6.6)	474 (85.5)
Was selection of predictors based on univariable analysis avoided?	355 (63.9)	0	200 (36.1)
Were complexities in the data (eg, censoring, competing risks, and sampling of control participants) accounted for appropriately?	0	5 (0.9)	550 (99.1)
Were relevant model performance measures evaluated appropriately?	0	0	555 (100.0)
Were model overfitting and optimism in model performance accounted for?	497 (89.5)	16 (2.8)	42 (7.7)
Did predictors and their assigned weights in the final model correspond to the results from the reported multivariable analysis?	53 (9.6)	0	502 (90.4)

Abbreviations: AI, artificial intelligence; PROBAST, Prediction Model Risk of Bias Assessment Tool; RCT, randomized clinical trial; ROB, risk of bias.

^a The criteria for answering the signaling questions largely adhered to the PROBAST but were slightly modified to fit the current study (eMethods 4 in Supplement 1).

Clinical Applicability Concerns in AI Models

In total, by using the PROBAST, a third of the models were assessed for high concerns about their clinical applicability in the predictors and outcome domains. High concern for clinical applicability in the participants domain was found for 2 of 555 models (0.4%; 95% CI, 0.00%-0.01%).^{26,31}

Furthermore, high concerns regarding clinical applicability were found for 199 of 555 models (35.9%; 95% CI, 31.9%-39.9%) in the predictors domain^{25, 33, 35, 37, 39, 41, 44, 45, 48, 53-57, 59, 60, 62, 78-81, 85, 89, 92, 99, 100, 104, 107, 113, 115, 117, 121, 122, 129, 130, 133, 135, 136, 148, 150, 154, 158, 160, 161, 167, 169, 170, 172, 173, 175, 178, 183, 190, 191, 193, 195, 197, 201, 204, 206, 207, 210, 212, 215, 216, 224, 225, 229, 232, 233, 235, 238, 240, 242, 247, 251, 253, 257, 260, 274, 277, 279, 283, 285, 286, 290, 295, 299, 303, 305-307, 312, 317-320, 322, 326, 332-336, 339, 340, 345, 347, 349-353, 357-360, 363-365, 376, 385, 388-393, 398, 400, 402-406, 409-411, 413, 415-418, 421, 423-426, 428-430, 433, 434, 441, 442, 444, 449-452, 458, 459, 461, 464, 466, 468, 472, 475, 478, 484, 488, 491, 493, 502, 504, 505, 516, 529, 532, 533, 537, 538, 540, 541}

and for 217 of 555 models (39.1%; 95% CI, 35.0%-43.2%) in the outcome domain.^{26, 32, 34-37, 39, 41, 44, 45, 48, 53-57, 59, 60, 62, 68, 69, 75, 78, 79, 81, 85, 89, 92, 99, 100, 104, 107, 113, 115-117, 121, 129, 130, 133, 135, 136, 148, 150, 154, 158, 160, 161, 167, 169, 170, 173, 175, 178, 183, 190, 191, 193, 195, 197, 201, 204, 206, 207, 210, 212, 215, 216, 224, 225, 229, 232-235, 238, 240, 242, 247, 251, 253, 257, 260, 274, 277, 279, 283, 285, 286, 288, 290, 295, 297-300, 303-308, 311, 315-320, 322, 326, 332-336, 339, 340, 343, 345, 347, 349-353, 357, 358, 360, 363-365, 367, 373, 376, 382, 385, 388-393, 398, 400, 402-406, 409-411, 413, 415-418, 420-426, 428-430, 433, 434, 436, 441, 442, 444, 446, 449, 451, 452, 459, 461, 464, 466, 468, 472, 475, 478, 484, 488, 491, 493, 502, 504, 505, 516, 520, 529, 532, 533, 537, 538, 540, 541}

In addition, none of these AI models were perceived to be applicable to clinical practice to date.

Reporting Quality of AI Models

Overall, all models were assessed for poor reporting quality based on the modified CLEAR statement. Reporting completeness (ie, number of reported items/number of total items) for these AI models was found to be insufficient at 61.2% (95% CI, 60.6%-61.8%). Full results for reporting quality are presented in **Table 2**.

All of the models showed overall poor reporting quality in the data domain across 13 signaling questions. Lack of reporting for how to handle out-of-distribution images was the main source of the poor reporting quality rating in the data domain. In addition, 378 of 555 models (68.1%; 95% CI, 64.2%-72.0%) lacked reports for quality control (eg, signaling question: was how to handle neuroimaging artifacts reported?), incurring a low reporting quality rating.^{27, 28, 31-33, 35-42, 46, 49-51, 53, 54, 56-58, 61, 63, 64, 68-78, 80, 87-91, 94, 96-98, 100, 101, 103, 105, 112-115, 121, 122, 125, 127, 129, 134, 137, 138, 141-144, 147, 149, 154-158, 160-162, 164, 165, 170-177, 179-182, 185-191, 193-196, 199, 203, 207, 209, 210, 214, 215, 217, 219, 222, 223, 226-239, 242-246, 248-261, 263-265, 268, 269, 271-284, 286-291, 293-295, 297-303, 305, 306, 308-315, 321, 323-327, 332-342, 344-347, 349, 351, 353, 355-358, 360-366, 368-370, 372-375, 377-380, 382-385, 387-392, 394-402, 404-407, 409-421, 425-430, 433-438, 440-447, 449-454, 457-467, 469, 471, 472, 475-477, 479-483, 485, 487, 489-494, 496-498, 501, 504, 508, 509, 511, 513-516, 518-520, 526, 528, 530-537, 539, 540} Overall, a mean 58.9% (95% CI, 58.0%-59.7%) of models required contents in the data domain.

Approximately half of the models (258 of 555 [46.48%; 95% CI, 42.3%-50.6%]) were assessed for poor reporting quality in the technique domain across 3 signaling questions.^{25, 28, 29, 33-35, 44, 45, 47-49, 51, 53, 54, 56, 59, 60, 62, 66, 73, 75, 78, 79, 81, 83, 84, 95, 99, 100, 107, 114, 117, 122, 124, 126, 128-131, 133, 135, 137, 142, 144-148, 151, 153, 155, 159, 161, 163, 165-167, 169, 171, 173, 174, 177, 179, 183, 184, 197, 199, 201-204, 206-208, 210-213, 216, 217, 221, 224, 225, 229, 231, 233-237, 243, 245-248, 253, 255, 257-259, 274, 275, 278, 279, 283-285, 288, 291, 294, 297, 299, 302, 304-307, 311, 314, 317-326, 328-331, 333-336, 339, 343-347, 350, 351, 353, 355, 357, 360-362, 364, 365, 372, 375, 376, 379, 382, 384, 385, 389, 390, 396, 399, 402-406, 413, 415-418, 420-425, 429-434, 436, 439-442, 445, 446, 448-453, 456, 464, 466, 470-476, 478, 480, 481, 486, 487, 492, 493, 495, 498, 500, 502-507, 509, 511, 513, 515, 516, 518, 521, 528-532, 535, 536, 539, 541} The unique source for the degraded reporting quality in this domain was the absence of algorithmic details, which limited reproducibility (eg, signaling question: were details for algorithm development reported?). The mean reporting completeness for these models in the technique domain was satisfied (84.5%; 95% CI, 83.1%-85.8%).

All models were rated for poor reporting quality in the technical assessment domain across 4 signaling questions. Of the 555 models, 544 (98.0%; 95% CI, 96.9%-99.2%) lacked reports for how to evaluate AI performance publicly.^{25-68, 70-127, 129-144, 146-178, 180-470, 472-479, 481, 483-501, 503-506, 508-536, 538-541} Additionally, the absence-of-bias assessment was associated with degraded reporting quality

in this domain (eg, signaling question: were bias assessments discussed?). Thus, the overall reporting completeness for these AI models was the poorest in the technical assessment domain (39.9%; 95% CI, 38.8%-41.1%).

One-hundred fifty of 555 models (27.0%; 95% CI, 23.3%-30.7%) were rated with poor reporting quality in the applications domain across 2 signaling questions.^{26, 28, 29, 32, 36, 38, 41, 45, 50, 51, 60, 65, 69, 74, 78, 82, 84, 94, 97, 99, 105, 107, 108, 112, 117, 119, 120, 125, 132-134, 138, 139, 141, 143, 146, 150, 159, 172, 183, 186, 190, 193, 194, 200, 203, 204, 214, 219, 220, 222, 223, 228-230, 232, 233, 241, 243, 244, 251, 257, 259-261, 263, 267, 269, 274, 280, 281, 284-286, 291, 293, 297, 298, 300, 301, 311-313, 315, 316, 321, 329, 337, 340, 343, 354, 361, 363, 369-371, 379, 392, 395, 397, 399, 405, 408, 411, 413, 418, 419, 422, 423, 432, 440, 445, 446, 448, 449, 456, 457, 461, 471, 473, 474, 476, 481, 484, 485, 490, 496, 506, 513, 514, 520, 527, 538-540} Lacking intrinsic reports or discussions of the clinical implications of these models was the main source of the poor rating in this domain (eg, signaling question: were use cases and target conditions discussed?). The mean overall reporting completeness in the applications domain was found to be favorable (84.6%; 95% CI, 81.8%-86.5%).

Table 2. Reporting Quality for All Included AI Models Using the Modified CLEAR (N = 555)

Signaling question ^a	Answers, No. (%)		
	Yes or probably yes	No information	No or probably no
Domain 1: data			
Were neuroimaging types reported?	555 (100.0)	0	0
Was how to handle neuroimaging artifacts reported?	177 (31.9)	0	378 (68.1)
Were technical acquisition details reported?	532 (95.9)	0	23 (4.1)
Were preprocessing procedures reported?	501 (90.0)	0	54 (10.0)
Was synthetic neuroimaging made public if used?	17 (3.1)	0	538 (96.9)
Were public neuroimages referenced adequately?	188 (33.9)	0	367 (66.1)
Were patient-level metadata reported enough (eg, geographic location, sex and gender distribution, and race and ethnicity), and how it was extracted?	362 (65.2)	0	193 (34.8)
Were potential biases from using patient information and metadata reported?	356 (64.2)	0	199 (35.8)
Were data set partition methods reported?	555 (100.0)	0	0
Were sample sizes for subsets (ie, training, validation, and test) reported?	555 (100.0)	0	0
Were external test sets reported?	87 (15.7)	0	468 (84.3)
Were class distributions and balance processes reported?	364 (65.6)	0	191 (34.4)
Were out-of-distribution neuroimages reported?	0	0	555 (100.0)
Domain 2: technique			
Were labeling methods reported appropriately?	555 (100.0)	0	0
Were references to common/accepted diagnostic labels reported?	555 (100.0)	0	0
Were details for algorithm development reported?	297 (53.5)	0	258 (46.5)
Domain 3: technical assessment			
Was how to publicly evaluate algorithm reported?	11 (2.0)	0	544 (98.0)
Were model performance measures reported?	555 (100.0)	0	0
Were benchmarking, technical comparison, and novelty discussed?	322 (58.0)	0	233 (42.0)
Were bias assessments discussed?	0	0	555 (100.0)
Domain 4: applications			
Were use cases and target conditions discussed?	529 (95.3)	0	26 (4.7)
Were potential impacts on the health care team and patients introduced?	405 (73.0)	0	150 (27.0)

Abbreviations: AI, artificial intelligence; CLEAR, Checklist for Evaluation of Image-Based Artificial Intelligence Reports; PROBAST, Prediction Model Risk of Bias Assessment Tool.

^a All items were translated from modified CLEAR statements into signaling questions that adhered to the PROBAST. Based on the PROBAST rating criteria, each domain was rated as poor reporting quality if 1 or more items were answered with *no* or *probably no*. Overall reporting quality was determined by rating for each item, with 1 or more items answered by *no* or *probably no* being poor reporting quality.

Discussion

Despite the tremendous potential for neuroimaging-based AI models in psychiatric research and clinical translation, the present study showed a high ROB that was associated with barriers to translation of the models into clinical application. To our surprise, the majority of models exhibited a high ROB. These models further exhibited low potential for both clinical and health care applicability based on the PROBAST. Thus, optimistic claims with respect to reliable AI-based psychiatric diagnosis should be considered with caution. Furthermore, poor reporting quality (with a mean reporting completeness of 61.2%) was found to be associated with additional barriers to clinical and practical translation of these models. Despite their high potential, the AI models presented to date do not fulfill the criteria for being recommended for use in psychiatric diagnostics, and several challenges remain on the way to translation.

In this study, we found that 83.1% of existing AI models exhibited a high ROB for psychiatric diagnosis. These findings align with results of a multivariable statistical model (eg, clinical prediction model [CPM]) for diagnosing both somatic and psychiatric disorders that showed 98% and 94% of the models, respectively, had a high ROB in diagnosis.^{12,545} In addition, high ROB was observed for prognostication of oral health (75% of models) and cardiovascular health (81% of models).^{546,547} Thus, compared with traditional statistical models, the current AI models did not fulfill the promise of superior technical (statistical) model merits (ie, unbiased prediction) in clinical practice. In addition, unlike neurological or physiological diseases with clear nosological landmarks, neuroimaging-based AI models may outperform traditional clinical models for psychiatric diagnosis only if these neuromarkers were associated with apparently differentiable actionability. This situation may be an additional source of high ROB in these models.

The main reason for incurring high ROB in these AI models was found in the analysis domain, especially the sample size and model configurations. Inadequate sample size represented a long-debated concern leading to inflated model performance in neuroimaging-based AI.^{8,9,548} Despite the ongoing debate, a sample of more than 200 participants for building AI models is increasingly becoming commonly acceptable.⁵⁴⁹⁻⁵⁵² However, about 80% of AI models for psychiatric diagnosis were trained on far smaller samples, leading to a high ROB and resulting in poor generalizability. On the other hand, model configurations, including data leakage, performance optimization, and absence of handling data complexities, represented key challenges to increasing model ROB. Data leakage, for instance, referred to the role that knowledge of outcome played in feature selection in the training set.⁵⁵³ Compared with traditional statistical models, the number of neuroimaging-based features (eg, voxel and functional connectivity) was large. For dimension reduction, univariate analysis was consistently used for feature selection in the whole data set, which made testing the data set no longer independent.^{9,551} In addition, unlike CPM, the data structure for AI models allows for a substantial variation in optimizing and turning parameters to manipulate performance.^{554,555} Fine-tuning the models may thus improve diagnostic performance, but such tailor-built configurations sacrifice generalizability for unseen patients.⁵⁵⁶ On balance, a high ROB in the analysis domain should be addressed to prompt clinical applications in future AI models.

Standardized and transparent reports for a clinical diagnostic model are increasingly advocated to improve clinical applicability and unbiased practice.^{557,558} However, we found that the reporting completeness following a benchmark assessment was only 61.2%, critically limiting replicability and applicability. The finding of insufficient reporting resonated with the study by Heus et al⁵⁵⁹ that found low overall reporting completeness (ie, 44%) for CPM across clinical domains. With regard to AI models for other clinical diseases, the reporting completeness was still approximately 50%.^{560,561} Going forward, complete and transparent reporting quality is imperative for applicable and feasible AI diagnostic models in clinical practice.

Taken together, a concise guideline that consists of 3 aspects is proposed in this study: (1) adopt appropriate reporting guidelines (eg, CLEAR) and benchmarks (eg, PROBAST-AI) before building models; (2) increase attention on the quality of models (eg, adequate sample size, rigorous calibration examination, and controls for data complexities); and (3) propel translational or accessible

diagnostic models (eg, report more details for technical assessments and access enough model materials for clinical validations or applications).

Limitations

This study has limitations. One limitation is the potential overestimation of ROB due to the lack of a suitable benchmark. Despite the extension of the PROBAST to AI models, the applicable version is pending.⁵⁶² Results of the current study could be validated by the PROBAST-AI when it becomes available. Similarly, the findings regarding the reporting quality of these models could be enriched by the development of a psychiatry-specific image-based AI model reporting checklist. A second limitation is the rating heterogeneity of the benchmarks we used. Although it had acceptable reliability, a certain assessment was found to have heterogeneity by assessors with specific expertise, especially in different assessment domains (eMethods 6 in [Supplement 1](#)). Thus, it would be highly beneficial if experts with interdisciplinary scientific training validated the findings by rating the AI models. A third limitation is that we did not test the models' clinical performance; thus, it is prudent for future studies to examine these models in clinical practice to determine their applicability.

Conclusions

In this systematic review of risks for available neuroimaging-based AI models for psychiatric diagnosis, most AI models had an overall high ROB, especially in the analysis domain. Furthermore, the overall reporting quality was poor, and the mean reporting completeness for these models was 61.2%. Existing AI models may not be as mature for direct clinical applications as is claimed given their high ROB and poor reporting quality. In the analysis domain, ROB in of AI diagnostic models should be addressed before clinical application.

ARTICLE INFORMATION

Accepted for Publication: January 15, 2023.

Published: March 6, 2023. doi:10.1001/jamanetworkopen.2023.1671

Open Access: This is an open access article distributed under the terms of the [CC-BY-NC-ND License](#). © 2023 Chen Z et al. *JAMA Network Open*.

Corresponding Author: Zhiyi Chen, PhD, (chenzhiyi@tmmu.edu.cn); and Zhengzhi Feng, PhD, MD (fzz@tmmu.edu.cn), Army Medical University, No. 30 Gao Tan-Yan Main St, Shapingba, Chongqing 400038, China.

Author Affiliations: School of Psychology, Third Military Medical University, Chongqing, China (Chen, X. Liu, Miao, Gong, Yu, Feng); Experimental Research Center for Medical and Psychological Science, Third Military Medical University, Chongqing, China (Chen, X. Liu, Miao, Gong, Feng); Department of Neurology, Daping Hospital, Third Military Medical University, Chongqing, China (Yang, Wang); Department of Psychology, Clark University, Worcester, Massachusetts (Leonov); School of Psychology, Qufu Normal University, Qufu, China (C. Liu); School of Psychology, Nanjing Normal University, Nanjing, China (Chuan-Peng).

Author Contributions: Dr Chen had full access to all of the data in the study and takes responsibility for the integrity of the data and the accuracy of the data analysis. Dr Chen and Ms X. Liu contributed equally to this work.

Concept and design: Chen, X. Liu, Wang, Zhengzhi.

Acquisition, analysis, or interpretation of data: Chen, X. Liu, Yang, Miao, Gong, Yu, Leonov, C. Liu, Chuan-Peng.

Drafting of the manuscript: Chen, X. Liu, Yang, Miao, Yu.

Critical revision of the manuscript for important intellectual content: Chen, Wang, Gong, Leonov, C. Liu, Zhengzhi, Chuan-Peng.

Statistical analysis: Chen, X. Liu, Miao, Gong, Yu.

Obtained funding: Zhengzhi.

Administrative, technical, or material support: Chen, X. Liu, Yang, Yu, C. Liu, Zhengzhi.

Supervision: Chen, Wang, Zhengzhi.

Conflict of Interest Disclosures: None reported.

Funding/Support: This work was funded by grant CWS20J007 from the Chinese People's Liberation Army (PLA) Key Research Foundation, grant 20220102 from the Army Medical University Academic Rising Star Foundation, and grant 2022160258 from PLA Talent Program Foundation.

Role of the Funder/Sponsor: The funders had a role in reviewing and approving this manuscript for publication. The funders had no role in the design and conduct of the study or the collection, management, analysis, and interpretation of the data.

Data Sharing Statement: See [Supplement 2](#).

REFERENCES

1. Sui J, Jiang R, Bustillo J, Calhoun V. Neuroimaging-based individualized prediction of cognition and behavior for mental disorders and health: methods and promises. *Biol Psychiatry*. 2020;88(11):818-828. doi:10.1016/j.biopsych.2020.02.016
2. Arbabshirani MR, Plis S, Sui J, Calhoun VD. Single subject prediction of brain disorders in neuroimaging: Promises and pitfalls. *Neuroimage*. 2017;145(Pt B):137-165. doi:10.1016/j.neuroimage.2016.02.079
3. Eyre HA, Singh AB, Reynolds C III. Tech giants enter mental health. *World Psychiatry*. 2016;15(1):21-22. doi:10.1002/wps.20297
4. Jordan MI, Mitchell TM. Machine learning: Trends, perspectives, and prospects. *Science*. 2015;349(6245):255-260. doi:10.1126/science.aaa8415
5. Yu JS, Xue AY, Redei EE, Bagheri N. A support vector machine model provides an accurate transcript-level-based diagnostic for major depressive disorder. *Transl Psychiatry*. 2016;6(10):e931. doi:10.1038/tp.2016.198
6. Hazlett HC, Gu H, Munsell BC, et al; IBIS Network; Clinical Sites; Data Coordinating Center; Image Processing Core; Statistical Analysis. Early brain development in infants at high risk for autism spectrum disorder. *Nature*. 2017;542(7641):348-351. doi:10.1038/nature21369
7. Lv J, Di Biase M, Cash RFH, et al. Individual deviations from normative models of brain structure in a large cross-sectional schizophrenia cohort. *Mol Psychiatry*. 2021;26(7):3512-3523. doi:10.1038/s41380-020-00882-5
8. Nielsen AN, Barch DM, Petersen SE, Schlaggar BL, Greene DJ. Machine learning with neuroimaging: evaluating its applications in psychiatry. *Biol Psychiatry Cogn Neurosci Neuroimaging*. 2020;5(8):791-798. doi:10.1016/j.bpsc.2019.11.007
9. Varoquaux G, Raamana PR, Engemann DA, Hoyos-Idrobo A, Schwartz Y, Thirion B. Assessing and tuning brain decoders: Cross-validation, caveats, and guidelines. *Neuroimage*. 2017;145(Pt B):166-179. doi:10.1016/j.neuroimage.2016.10.038
10. Roberts M, Driggs D, Thorpe M, et al. Common pitfalls and recommendations for using machine learning to detect and prognosticate for COVID-19 using chest radiographs and CT scans. *Nat Mach Intell*. 2021;3:199-217. doi:10.1038/s42256-021-00307-0
11. Wynants L, Van Calster B, Collins GS, et al. Prediction models for diagnosis and prognosis of Covid-19: systematic review and critical appraisal. *BMJ*. 2020;369:m1328. doi:10.1136/bmj.m1328
12. Andaur Navarro CL, Damen JAA, Takada T, et al. Risk of bias in studies on prediction models developed using supervised machine learning techniques: systematic review. *BMJ*. 2021;375(2281):n2281. doi:10.1136/bmj.n2281
13. Meehan AJ, Lewis SJ, Fazel S, et al. Clinical prediction models in psychiatry: a systematic review of two decades of progress and challenges. *Mol Psychiatry*. 2022;27(6):2700-2708. doi:10.1038/s41380-022-01528-4
14. Walter M, Alizadeh S, Jamalabadi H, et al. Translational machine learning for psychiatric neuroimaging. *Prog Neuropsychopharmacol Biol Psychiatry*. 2019;91:113-121. doi:10.1016/j.pnpbp.2018.09.014
15. Bzdok D, Meyer-Lindenberg A. Machine learning for precision psychiatry: opportunities and challenges. *Biol Psychiatry Cogn Neurosci Neuroimaging*. 2018;3(3):223-230. doi:10.1016/j.bpsc.2017.11.007
16. Vasey B, Nagendran M, Campbell B, et al; DECIDE-AI expert group. Reporting guideline for the early-stage clinical evaluation of decision support systems driven by artificial intelligence: DECIDE-AI. *Nat Med*. 2022;28(5):924-933. doi:10.1038/s41591-022-01772-9
17. Bossuyt PM, Reitsma JB, Bruns DE, et al; Standards for Reporting of Diagnostic Accuracy. Towards complete and accurate reporting of studies of diagnostic accuracy: the STARD initiative. *BMJ*. 2003;326(7379):41-44. doi:10.1136/bmj.326.7379.41
18. Collins GS, Reitsma JB, Altman DG, Moons KG. Transparent Reporting of a Multivariable Prediction Model for Individual Prognosis or Diagnosis (TRIPOD): the TRIPOD statement. *BMJ*. 2015;350:g7594. doi:10.1136/bmj.g7594

19. Lu JH, Callahan A, Patel BS, et al. Assessment of adherence to reporting guidelines by commonly used clinical prediction models from a single vendor: a systematic review. *JAMA Netw Open*. 2022;5(8):e2227779. doi:10.1001/jamanetworkopen.2022.27779
20. Glasziou P, Altman DG, Bossuyt P, et al. Reducing waste from incomplete or unusable reports of biomedical research. *Lancet*. 2014;383(9913):267-276. doi:10.1016/S0140-6736(13)62228-X
21. Cai R, Wu X, Li C, Chao J. Prediction models for cardiovascular disease risk in the hypertensive population: a systematic review. *J Hypertens*. 2020;38(9):1632-1639. doi:10.1097/HJH.0000000000002442
22. Nagendran M, Chen Y, Lovejoy CA, et al. Artificial intelligence versus clinicians: systematic review of design, reporting standards, and claims of deep learning studies. *BMJ*. 2020;368:m689. doi:10.1136/bmj.m689
23. Daneshjou R, Barata C, Betz-Stablein B, et al. Checklist for evaluation of image-based artificial intelligence reports in dermatology: CLEAR Derm consensus guidelines from the International Skin Imaging Collaboration Artificial Intelligence Working Group. *JAMA Dermatol*. 2022;158(1):90-96. doi:10.1001/jamadermatol.2021.4915
24. Wolff RF, Moons KGM, Riley RD, et al; PROBAST Group. PROBAST: a tool to assess the risk of bias and applicability of prediction model studies. *Ann Intern Med*. 2019;170(1):51-58. doi:10.7326/M18-1376
25. Knoth IS, Lajnef T, Rigoulot S, et al. Auditory repetition suppression alterations in relation to cognitive functioning in fragile X syndrome: a combined EEG and machine learning approach. *J Neurodev Disord*. 2018;10(1):4. doi:10.1186/s11689-018-9223-3
26. Pedersen M, Curwood EK, Archer JS, Abbott DF, Jackson GD. Brain regions with abnormal network properties in severe epilepsy of Lennox-Gastaut phenotype: multivariate analysis of task-free fMRI. *Epilepsia*. 2015;56(11):1767-1773. doi:10.1111/epi.13135
27. Wang Y, Yuan L, Shi J, et al. Applying tensor-based morphometry to parametric surfaces can improve MRI-based disease diagnosis. *Neuroimage*. 2013;74:209-230. doi:10.1016/j.neuroimage.2013.02.011
28. Hoeft F, Walter E, Lightbody AA, et al. Neuroanatomical differences in toddler boys with fragile x syndrome and idiopathic autism. *Arch Gen Psychiatry*. 2011;68(3):295-305. doi:10.1001/archgenpsychiatry.2010.153
29. Parisot S, Ktena SI, Ferrante E, et al. Disease prediction using graph convolutional networks: application to autism spectrum disorder and Alzheimer's disease. *Med Image Anal*. 2018;48:117-130. doi:10.1016/j.media.2018.06.001
30. Matlis S, Boric K, Chu CJ, Kramer MA. Robust disruptions in electroencephalogram cortical oscillations and large-scale functional networks in autism. *BMC Neurol*. 2015;15:97. doi:10.1186/s12883-015-0355-8
31. Ingalhalikar M, Parker D, Bloy L, Roberts TP, Verma R. Diffusion based abnormality markers of pathology: toward learned diagnostic prediction of ASD. *Neuroimage*. 2011;57(3):918-927. doi:10.1016/j.neuroimage.2011.05.023
32. Shahamat H, Saniee Abadeh M. Brain MRI analysis using a deep learning based evolutionary approach. *Neural Netw*. 2020;126:218-234. doi:10.1016/j.neunet.2020.03.017
33. Bajestani GS, Behrooz M, Khani AG, Nouri-Baygi M, Mollaei A. Diagnosis of autism spectrum disorder based on complex network features. *Comput Methods Programs Biomed*. 2019;177:277-283. doi:10.1016/j.cmpb.2019.06.006
34. Lanka P, Rangaprakash D, Dretsch MN, Katz JS, Denney TS Jr, Deshpande G. Supervised machine learning for diagnostic classification from large-scale neuroimaging datasets. *Brain Imaging Behav*. 2020;14(6):2378-2416. doi:10.1007/s11682-019-00191-8
35. Zhang L, Wang XH, Li L. Diagnosing autism spectrum disorder using brain entropy: a fast entropy method. *Comput Methods Programs Biomed*. 2020;190:105240. doi:10.1016/j.cmpb.2019.105240
36. Rakić M, Cabezas M, Kushibar K, Oliver A, Lladó X. Improving the detection of autism spectrum disorder by combining structural and functional MRI information. *Neuroimage Clin*. 2020;25:102181. doi:10.1016/j.nicl.2020.102181
37. Ahmadiou M, Adeli H, Adeli A. Fractality and a wavelet-chaos-neural network methodology for EEG-based diagnosis of autistic spectrum disorder. *J Clin Neurophysiol*. 2010;27(5):328-333. doi:10.1097/WNP.0b013e3181f40dc8
38. Libero LE, DeRamus TP, Lahti AC, Deshpande G, Kana RK. Multimodal neuroimaging based classification of autism spectrum disorder using anatomical, neurochemical, and white matter correlates. *Cortex*. 2015;66:46-59. doi:10.1016/j.cortex.2015.02.008
39. Pham TH, Vicnesh J, Wei JKE, et al. Autism spectrum disorder diagnostic system using HOS bispectrum with EEG signals. *Int J Environ Res Public Health*. 2020;17(3):971. doi:10.3390/ijerph17030971

40. Graa O, Rezik I. Multi-view learning-based data proliferator for boosting classification using highly imbalanced classes. *J Neurosci Methods*. 2019;327:108344. doi:10.1016/j.jneumeth.2019.108344
41. Ingälhalikar M, Smith AR, Bloy L, Gur R, Roberts TPL, Verma R. Identifying sub-populations via unsupervised cluster analysis on multi-edge similarity graphs. In: Ayache N, Delingette H, Golland P, Mori K, eds. *Medical Image Computing and Computer-Assisted Intervention—MICCAI 2012. MICCAI 2012. Lecture Notes in Computer Science*. Vol 7511. Springer; 2012:254-261.
42. Khosla M, Jamison K, Kuceyeski A, Sabuncu MR. Ensemble learning with 3D convolutional neural networks for functional connectome-based prediction. *Neuroimage*. 2019;199:651-662. doi:10.1016/j.neuroimage.2019.06.012
43. Li H, Parikh NA, He L. A novel transfer learning approach to enhance deep neural network classification of brain functional connectomes. *Front Neurosci*. 2018;12:491. doi:10.3389/fnins.2018.00491
44. Sen B, Borle NC, Greiner R, Brown MRG. A general prediction model for the detection of ADHD and autism using structural and functional MRI. *PLoS One*. 2018;13(4):e0194856. doi:10.1371/journal.pone.0194856
45. Xu L, Hua Q, Yu J, Li J. Classification of autism spectrum disorder based on sample entropy of spontaneous functional near infra-red spectroscopy signal. *Clin Neurophysiol*. 2020;131(6):1365-1374. doi:10.1016/j.clinph.2019.12.400
46. Ma X, Wang XH, Li L. Identifying individuals with autism spectrum disorder based on the principal components of whole-brain phase synchrony. *Neurosci Lett*. 2021;742:135519. doi:10.1016/j.neulet.2020.135519
47. Rakhimberdina Z, Liu X, Murata AT. Population graph-based multi-model ensemble method for diagnosing autism spectrum disorder. *Sensors (Basel)*. 2020;20(21):6001. doi:10.3390/s20216001
48. Tsiaras V, Simos PG, Rezaie R, et al. Extracting biomarkers of autism from MEG resting-state functional connectivity networks. *Comput Biol Med*. 2011;41(12):1166-1177. doi:10.1016/j.combiomed.2011.04.004
49. Wang H, Chen C, Fushing H. Extracting multiscale pattern information of fMRI based functional brain connectivity with application on classification of autism spectrum disorders. *PLoS One*. 2012;7(10):e45502. doi:10.1371/journal.pone.0045502
50. Hu J, Cao L, Li T, Liao B, Dong S, Li P. Interpretable learning approaches in resting-state functional connectivity analysis: the case of autism spectrum disorder. *Comput Math Methods Med*. 2020;2020:1394830. doi:10.1155/2020/1394830
51. Jung M, Tu Y, Park J, et al. Surface-based shared and distinct resting functional connectivity in attention-deficit hyperactivity disorder and autism spectrum disorder. *Br J Psychiatry*. 2019;214(6):339-344. doi:10.1192/bjp.2018.248
52. Heinsfeld AS, Franco AR, Craddock RC, Buchweitz A, Meneguzzi F. Identification of autism spectrum disorder using deep learning and the ABIDE dataset. *Neuroimage Clin*. 2017;17:16-23. doi:10.1016/j.nicl.2017.08.017
53. Bhaumik R, Pradhan A, Das S, Bhaumik DK. Predicting autism spectrum disorder using domain-adaptive cross-site evaluation. *Neuroinformatics*. 2018;16(2):197-205. doi:10.1007/s12021-018-9366-0
54. Wang L, Wee CY, Tang X, Yap PT, Shen D. Multi-task feature selection via supervised canonical graph matching for diagnosis of autism spectrum disorder. *Brain Imaging Behav*. 2016;10(1):33-40. doi:10.1007/s11682-015-9360-1
55. Ecker C, Rocha-Rego V, Johnston P, et al; MRC AIMS Consortium. Investigating the predictive value of whole-brain structural MR scans in autism: a pattern classification approach. *Neuroimage*. 2010;49(1):44-56. doi:10.1016/j.neuroimage.2009.08.024
56. Payabvash S, Palacios EM, Owen JP, et al. White matter connectome edge density in children with autism spectrum disorders: potential imaging biomarkers using machine-learning models. *Brain Connect*. 2019;9(2):209-220. doi:10.1089/brain.2018.0658
57. Price T, Wee CY, Gao W, Shen D. Multiple-network classification of childhood autism using functional connectivity dynamics. In: Golland P, Hata N, Barillot C, Hornegger J, Howe R, eds. *Medical Image Computing and Computer-Assisted Intervention—MICCAI 2014. MICCAI 2014. Lecture Notes in Computer Science*. Vol 8675. Springer, Cham; 2014:177-184.
58. Haweel R, Shalaby A, Mahmoud A, et al. A robust DWT-CNN-based CAD system for early diagnosis of autism using task-based fMRI. *Med Phys*. 2021;48(5):2315-2326. doi:10.1002/mp.14692
59. Chen CP, Keown CL, Jahedi A, et al. Diagnostic classification of intrinsic functional connectivity highlights somatosensory, default mode, and visual regions in autism. *Neuroimage Clin*. 2015;8:238-245. doi:10.1016/j.nicl.2015.04.002
60. Anderson JS, Nielsen JA, Froehlich AL, et al. Functional connectivity magnetic resonance imaging classification of autism. *Brain*. 2011;134(Pt 12):3742-3754. doi:10.1093/brain/awr263

61. Uddin LQ, Supekar K, Lynch CJ, et al. Salience network-based classification and prediction of symptom severity in children with autism. *JAMA Psychiatry*. 2013;70(8):869-879. doi:10.1001/jamapsychiatry.2013.104
62. Nielsen JA, Zielinski BA, Fletcher PT, et al. Multisite functional connectivity MRI classification of autism: ABIDE results. *Front Hum Neurosci*. 2013;7:599. doi:10.3389/fnhum.2013.00599
63. Jahedi A, Nasamran CA, Faires B, Fan J, Müller RA. Distributed intrinsic functional connectivity patterns predict diagnostic status in large autism cohort. *Brain Connect*. 2017;7(8):515-525. doi:10.1089/brain.2017.0496
64. Retico A, Giuliano A, Tancredi R, et al. The effect of gender on the neuroanatomy of children with autism spectrum disorders: a support vector machine case-control study. *Mol Autism*. 2016;7:5. doi:10.1186/s13229-015-0067-3
65. Calderoni S, Retico A, Biagi L, Tancredi R, Muratori F, Tosetti M. Female children with autism spectrum disorder: an insight from mass-univariate and pattern classification analyses. *Neuroimage*. 2012;59(2):1013-1022. doi:10.1016/j.neuroimage.2011.08.070
66. Yamagata B, Itahashi T, Fujino J, et al. Machine learning approach to identify a resting-state functional connectivity pattern serving as an endophenotype of autism spectrum disorder. *Brain Imaging Behav*. 2019;13(6):1689-1698. doi:10.1007/s11682-018-9973-2
67. Gori I, Giuliano A, Muratori F, et al. Gray matter alterations in young children with autism spectrum disorders: comparing morphometry at the voxel and regional level. *J Neuroimaging*. 2015;25(6):866-874. doi:10.1111/jon.12280
68. Leming M, Górriz JM, Suckling J. Ensemble deep learning on large, mixed-site fMRI datasets in autism and other tasks. *Int J Neural Syst*. 2020;30(7):2050012. doi:10.1142/S0129065720500124
69. Shen MD, Nordahl CW, Li DD, et al. Extra-axial cerebrospinal fluid in high-risk and normal-risk children with autism aged 2-4 years: a case-control study. *Lancet Psychiatry*. 2018;5(11):895-904. doi:10.1016/S2215-0366(18)30294-3
70. Grossi E, Olivieri C, Buscema M. Diagnosis of autism through EEG processed by advanced computational algorithms: a pilot study. *Comput Methods Programs Biomed*. 2017;142:73-79. doi:10.1016/j.cmpb.2017.02.002
71. Gupta S, Rajapakse JC, Welsch RE; Alzheimer's Disease Neuroimaging Initiative. Ambivert degree identifies crucial brain functional hubs and improves detection of Alzheimer's disease and autism spectrum disorder. *Neuroimage Clin*. 2020;25:102186. doi:10.1016/j.nicl.2020.102186
72. Ghiassian S, Greiner R, Jin P, Brown MR. Using functional or structural magnetic resonance images and personal characteristic data to identify ADHD and autism. *PLoS One*. 2016;11(12):e0166934. doi:10.1371/journal.pone.0166934
73. Zu C, Gao Y, Munsell B, et al. Identifying disease-related subnetwork connectome biomarkers by sparse hypergraph learning. *Brain Imaging Behav*. 2019;13(4):879-892. doi:10.1007/s11682-018-9899-8
74. Katuwal GJ, Baum SA, Cahill ND, Michael AM. Divide and conquer: sub-grouping of ASD improves ASD detection based on brain morphometry. *PLoS One*. 2016;11(4):e0153331. doi:10.1371/journal.pone.0153331
75. Li Q, Becker B, Jiang X, et al. Decreased interhemispheric functional connectivity rather than corpus callosum volume as a potential biomarker for autism spectrum disorder. *Cortex*. 2019;119:258-266. doi:10.1016/j.cortex.2019.05.003
76. Dekhil O, Hajjdiab H, Shalaby A, et al. Using resting state functional MRI to build a personalized autism diagnosis system. *PLoS One*. 2018;13(10):e0206351. doi:10.1371/journal.pone.0206351
77. Yamagata B, Itahashi T, Fujino J, et al. Cortical surface architecture endophenotype and correlates of clinical diagnosis of autism spectrum disorder. *Psychiatry Clin Neurosci*. 2019;73(7):409-415. doi:10.1111/pcn.12854
78. Iidaka T. Resting state functional magnetic resonance imaging and neural network classified autism and control. *Cortex*. 2015;63:55-67. doi:10.1016/j.cortex.2014.08.011
79. Jamal W, Das S, Oprescu IA, Maharatna K, Apicella F, Sicca F. Classification of autism spectrum disorder using supervised learning of brain connectivity measures extracted from synchrostates. *J Neural Eng*. 2014;11(4):046019. doi:10.1088/1741-2560/11/4/046019
80. Zhang F, Savadjiev P, Cai W, et al. Whole brain white matter connectivity analysis using machine learning: an application to autism. *Neuroimage*. 2018;172:826-837. doi:10.1016/j.neuroimage.2017.10.029
81. Sujit SJ, Coronado I, Kamali A, Narayana PA, Gabr RE. Automated image quality evaluation of structural brain MRI using an ensemble of deep learning networks. *J Magn Reson Imaging*. 2019;50(4):1260-1267. doi:10.1002/jmri.26693

82. Huang H, Liu X, Jin Y, Lee SW, Wee CY, Shen D. Enhancing the representation of functional connectivity networks by fusing multi-view information for autism spectrum disorder diagnosis. *Hum Brain Mapp.* 2019;40(3):833-854. doi:10.1002/hbm.24415
83. Eill A, Jahedi A, Gao Y, et al. Functional connectivities are more informative than anatomical variables in diagnostic classification of autism. *Brain Connect.* 2019;9(8):604-612. doi:10.1089/brain.2019.0689
84. Xiao X, Fang H, Wu J, et al. Diagnostic model generated by MRI-derived brain features in toddlers with autism spectrum disorder. *Autism Res.* 2017;10(4):620-630. doi:10.1002/aur.1711
85. Kam TE, Suk HI, Lee SW. Multiple functional networks modeling for autism spectrum disorder diagnosis. *Hum Brain Mapp.* 2017;38(11):5804-5821. doi:10.1002/hbm.23769
86. Ktena SI, Parisot S, Ferrante E, et al. Metric learning with spectral graph convolutions on brain connectivity networks. *Neuroimage.* 2018;169:431-442. doi:10.1016/j.neuroimage.2017.12.052
87. Aghdam MA, Sharifi A, Pedram MM. Diagnosis of autism spectrum disorders in young children based on resting-state functional magnetic resonance imaging data using convolutional neural networks. *J Digit Imaging.* 2019;32(6):899-918. doi:10.1007/s10278-019-00196-1
88. Sadeghi M, Khosrowabadi R, Bakouie F, Mahdavi H, Eslahchi C, Pouretamad H. Screening of autism based on task-free fMRI using graph theoretical approach. *Psychiatry Res Neuroimaging.* 2017;263:48-56. doi:10.1016/j.pscychresns.2017.02.004
89. Chaddad A, Desrosiers C, Hassan L, Tanougast C. Hippocampus and amygdala radiomic biomarkers for the study of autism spectrum disorder. *BMC Neurosci.* 2017;18(1):52. doi:10.1186/s12868-017-0373-0
90. Djemal R, AlSharabi K, Ibrahim S, Alsuwailam A. EEG-based computer aided diagnosis of autism spectrum disorder using wavelet, entropy, and ANN. *Biomed Res Int.* 2017;2017:9816591. doi:10.1155/2017/9816591
91. Yahata N, Morimoto J, Hashimoto R, et al. A small number of abnormal brain connections predicts adult autism spectrum disorder. *Nat Commun.* 2016;7:11254. doi:10.1038/ncomms11254
92. Heunis T, Aldrich C, Peters JM, et al. Recurrence quantification analysis of resting state EEG signals in autism spectrum disorder: a systematic methodological exploration of technical and demographic confounders in the search for biomarkers. *BMC Med.* 2018;16(1):101. doi:10.1186/s12916-018-1086-7
93. Chen H, Duan X, Liu F, et al. Multivariate classification of autism spectrum disorder using frequency-specific resting-state functional connectivity: a multi-center study. *Prog Neuropsychopharmacol Biol Psychiatry.* 2016; 64:1-9. doi:10.1016/j.pnpbp.2015.06.014
94. Just MA, Cherkassky VL, Buchweitz A, Keller TA, Mitchell TM. Identifying autism from neural representations of social interactions: neurocognitive markers of autism. *PLoS One.* 2014;9(12):e113879. doi:10.1371/journal.pone.0113879
95. Akhavan Aghdam M, Sharifi A, Pedram MM. Combination of rs-fMRI and sMRI data to discriminate autism spectrum disorders in young children using deep belief network. *J Digit Imaging.* 2018;31(6):895-903. doi:10.1007/s10278-018-0093-8
96. Alturki FA, AlSharabi K, Abdurraqueeb AM, Aljalal M. EEG signal analysis for diagnosing neurological disorders using discrete wavelet transform and intelligent techniques. *Sensors (Basel).* 2020;20(9):2505. doi:10.3390/s20092505
97. Spiegel A, Mentch J, Haskins AJ, Robertson CE. Slower binocular rivalry in the autistic brain. *Curr Biol.* 2019;29(17):2948-2953.e3. doi:10.1016/j.cub.2019.07.026
98. Conti E, Retico A, Palumbo L, et al. Autism spectrum disorder and childhood apraxia of speech: early language-related hallmarks across structural MRI study. *J Pers Med.* 2020;10(4):275. doi:10.3390/jpm10040275
99. Bi XA, Liu Y, Jiang Q, Shu Q, Sun Q, Dai J. The diagnosis of autism spectrum disorder based on the random neural network cluster. *Front Hum Neurosci.* 2018;12:257. doi:10.3389/fnhum.2018.00257
100. Pollonini L, Patidar U, Situ N, Rezaie R, Papanicolaou AC, Zouridakis G. Functional connectivity networks in the autistic and healthy brain assessed using Granger causality. *Annu Int Conf IEEE Eng Med Biol Soc.* 2010;2010:1730-1733. doi:10.1109/IEMBS.2010.5626702
101. Eldridge J, Lane AE, Belkin M, Dennis S. Robust features for the automatic identification of autism spectrum disorder in children. *J Neurodev Disord.* 2014;6(1):12. doi:10.1186/1866-1955-6-12
102. Khan NA, Waheeb SA, Riaz A, Shang X. A three-stage teacher, student neural networks and sequential feed forward selection-based feature selection approach for the classification of autism spectrum disorder. *Brain Sci.* 2020;10(10):754. doi:10.3390/brainsci10100754
103. Sherkatghanad Z, Akhondzadeh M, Salari S, et al. Automated detection of autism spectrum disorder using a convolutional neural network. *Front Neurosci.* 2020;13:1325. doi:10.3389/fnins.2019.01325

104. Gao J, Chen M, Li Y, et al. Multisite autism spectrum disorder classification using convolutional neural network classifier and individual morphological brain networks. *Front Neurosci*. 2021;14:629630. doi:10.3389/fnins.2020.629630
105. Liu Y, Xu L, Li J, Yu J, Yu X. Attentional connectivity-based prediction of autism using heterogeneous rs-fMRI data from CC200 atlas. *Exp Neurol*. 2020;29(1):27-37. doi:10.5607/en.2020.29.1.27
106. Yang M, Cao M, Chen Y, et al. Large-scale brain functional network integration for discrimination of autism using a 3-D deep learning model. *Front Hum Neurosci*. 2021;15:687288. doi:10.3389/fnhum.2021.687288
107. Huang ZA, Zhu Z, Yau CH, Tan KC. Identifying autism spectrum disorder from resting-state fMRI using deep belief network. *IEEE Trans Neural Netw Learn Syst*. 2021;32(7):2847-2861. doi:10.1109/TNNLS.2020.3007943
108. Zhao J, Song J, Li X, Kang J. A study on EEG feature extraction and classification in autistic children based on singular spectrum analysis method. *Brain Behav*. 2020;10(12):e01721. doi:10.1002/brb3.1721
109. Almuqhim F, Saeed F. ASD-SAENet: a sparse autoencoder, and deep-neural network model for detecting autism spectrum disorder (ASD) using fMRI data. *Front Comput Neurosci*. 2021;15:654315. doi:10.3389/fncom.2021.654315
110. Xu L, Sun Z, Xie J, Yu J, Li J, Wang J. Identification of autism spectrum disorder based on short-term spontaneous hemodynamic fluctuations using deep learning in a multi-layer neural network. *Clin Neurophysiol*. 2021;132(2):457-468. doi:10.1016/j.clinph.2020.11.037
111. Lu J, Kishida K, De Asis Cruz J, et al. Single stimulus fMRI produces a neural individual difference measure for autism spectrum disorder. *Clin Psychol Sci*. 2015;3(3):422-432. doi:10.1177/2167702614562042
112. Ahmed MR, Zhang Y, Liu Y, Liao H. Single volume image generator and deep learning-based ASD classification. *IEEE J Biomed Health Inform*. 2020;24(11):3044-3054. doi:10.1109/JBHI.2020.2998603
113. Xu L, Geng X, He X, Li J, Yu J. Prediction in autism by deep learning short-time spontaneous Hemodynamic fluctuations. *Front Neurosci*. 2019;13:1120. doi:10.3389/fnins.2019.01120
114. Wee CY, Wang L, Shi F, Yap PT, Shen D. Diagnosis of autism spectrum disorders using regional and interregional morphological features. *Hum Brain Mapp*. 2014;35(7):3414-3430. doi:10.1002/hbm.22411
115. Sewani H, Kashef R. An autoencoder-based deep learning classifier for efficient diagnosis of autism. *Children (Basel)*. 2020;7(10):182. doi:10.3390/children7100182
116. Shi C, Xin X, Zhang J. Domain adaptation using a three-way decision improves the identification of autism patients from multisite fMRI data. *Brain Sci*. 2021;11(5):603. doi:10.3390/brainsci11050603
117. Kazeminejad A, Sotero RC. The importance of anti-correlations in graph theory based classification of autism spectrum disorder. *Front Neurosci*. 2020;14:676. doi:10.3389/fnins.2020.00676
118. Yin W, Mostafa S, Wu FX. Diagnosis of autism spectrum disorder based on functional brain networks with deep learning. *J Comput Biol*. 2021;28(2):146-165. doi:10.1089/cmb.2020.0252
119. Jiao Y, Chen R, Ke X, Chu K, Lu Z, Herskovits EH. Predictive models of autism spectrum disorder based on brain regional cortical thickness. *Neuroimage*. 2010;50(2):589-599. doi:10.1016/j.neuroimage.2009.12.047
120. Murdaugh DL, Shinkareva SV, Deshpande HR, Wang J, Pennick MR, Kana RK. Differential deactivation during mentalizing and classification of autism based on default mode network connectivity. *PLoS One*. 2012;7(11):e50064. doi:10.1371/journal.pone.0050064
121. Song Y, Epalle TM, Lu H. Characterizing and predicting autism spectrum disorder by performing resting-state functional network community pattern analysis. *Front Hum Neurosci*. 2019;13:203. doi:10.3389/fnhum.2019.00203
122. Irimia A, Lei X, Torgerson CM, Jacokes ZJ, Abe S, Van Horn JD. Support vector machines, multidimensional scaling and magnetic resonance imaging reveal structural brain abnormalities associated with the interaction between autism spectrum disorder and sex. *Front Comput Neurosci*. 2018;12:93. doi:10.3389/fncom.2018.00093
123. Eslami T, Mirjalili V, Fong A, Laird AR, Saeed F. ASD-DiagNet: a hybrid learning approach for detection of autism spectrum disorder using fMRI data. *Front Neuroinform*. 2019;13:70. doi:10.3389/fninf.2019.00070
124. Sarovic D, Hadjikhani N, Schneiderman J, Lundström S, Gillberg C. Autism classified by magnetic resonance imaging: a pilot study of a potential diagnostic tool. *Int J Methods Psychiatr Res*. 2020;29(4):1-18. doi:10.1002/mp.1846
125. Kazeminejad A, Sotero RC. Topological properties of resting-state fMRI functional networks improve machine learning-based autism classification. *Front Neurosci*. 2019;12:1018. doi:10.3389/fnins.2018.01018
126. Guo X, Dominick KC, Minai AA, Li H, Erickson CA, Lu LJ. Diagnosing autism spectrum disorder from brain resting-state functional connectivity patterns using a deep neural network with a novel feature selection method. *Front Neurosci*. 2017;11:460. doi:10.3389/fnins.2017.00460

127. Thomas RM, Gallo S, Cerliani L, Zhutovsky P, El-Gazzar A, van Wingen G. Classifying autism spectrum disorder using the temporal statistics of resting-state functional MRI data with 3D convolutional neural networks. *Front Psychiatry*. 2020;11:440. doi:10.3389/fpsy.2020.00440
128. Li X, Zhou Y, Dvornek N, et al. BrainGNN: interpretable brain graph neural network for fMRI analysis. *Med Image Anal*. 2021;74:102233. doi:10.1016/j.media.2021.102233
129. Wang Z, Peng D, Shang Y, Gao J. Autistic spectrum disorder detection and structural biomarker identification using self-attention model and individual-level morphological covariance brain networks. *Front Neurosci*. 2021;15:756868. doi:10.3389/fnins.2021.756868
130. Haweel R, Seada N, Ghoniemy S, Alghamdi NS, El-Baz A. A CNN deep local and global ASD classification approach with continuous wavelet transform using task-based fMRI. *Sensors (Basel)*. 2021;21(17):5822. doi:10.3390/s21175822
131. Squarcina L, Nosari G, Marin R, et al. Automatic classification of autism spectrum disorder in children using cortical thickness and support vector machine. *Brain Behav*. 2021;11(8):e2238. doi:10.1002/brb3.2238
132. Baygin M, Dogan S, Tuncer T, et al. Automated ASD detection using hybrid deep lightweight features extracted from EEG signals. *Comput Biol Med*. 2021;134:104548. doi:10.1016/j.combiomed.2021.104548
133. Yang C, Wang P, Tan J, Liu Q, Li X. Autism spectrum disorder diagnosis using graph attention network based on spatial-constrained sparse functional brain networks. *Comput Biol Med*. 2021;139:104963. doi:10.1016/j.combiomed.2021.104963
134. Elnakieb Y, Ali MT, Elnakib A, et al. The role of diffusion tensor MR imaging (DTI) of the brain in diagnosing autism spectrum disorder: promising results. *Sensors (Basel)*. 2021;21(24):8171. doi:10.3390/s21248171
135. Okamoto N, Akama H. Extended invariant information clustering is effective for leave-one-site-out cross-validation in resting state functional connectivity modeling. *Front Neuroinform*. 2021;15:709179. doi:10.3389/fninf.2021.709179
136. Liao M, Duan H, Wang G. Application of machine learning techniques to detect the children with autism spectrum disorder. *J Healthc Eng*. 2022;2022:9340027. doi:10.1155/2022/9340027
137. Wang N, Yao D, Ma L, Liu M. Multi-site clustering and nested feature extraction for identifying autism spectrum disorder with resting-state fMRI. *Med Image Anal*. 2022;75:102279. doi:10.1016/j.media.2021.102279
138. Guo X, Wang J, Wang X, et al. Diagnosing autism spectrum disorder in children using conventional MRI and apparent diffusion coefficient based deep learning algorithms. *Eur Radiol*. 2022;32(2):761-770. doi:10.1007/s00330-021-08239-4
139. Gao K, Fan Z, Su J, et al. Deep transfer learning for cerebral cortex using area-preserving geometry mapping. *Cereb Cortex*. 2022;32(14):2972-2984. doi:10.1093/cercor/bhab394
140. Zhao L, Sun YK, Xue SW, Luo H, Lu XD, Zhang LH. Identifying boys with autism spectrum disorder based on whole-brain resting-state interregional functional connections using a boruta-based support vector machine approach. *Front Neuroinform*. 2022;16:761942. doi:10.3389/fninf.2022.761942
141. Shao L, Fu C, You Y, Fu D. Classification of ASD based on fMRI data with deep learning. *Cogn Neurodyn*. 2021;15(6):961-974. doi:10.1007/s11571-021-09683-0
142. Li L, Jiang H, Wen G, et al. TE-HI-GCN: an ensemble of transfer hierarchical graph convolutional networks for disorder diagnosis. *Neuroinformatics*. 2022;20(2):353-375. doi:10.1007/s12021-021-09548-1
143. Germann J, Gouveia FV, Brentani H, et al. Involvement of the habenula in the pathophysiology of autism spectrum disorder. *Sci Rep*. 2021;11(1):21168. doi:10.1038/s41598-021-00603-0
144. Kang J, Jin Y, Liang G, Li X. Accurate assessment of low-function autistic children based on EEG feature fusion. *J Clin Neurosci*. 2021;90:351-358. doi:10.1016/j.jocn.2021.06.022
145. Peng L, Liu X, Ma D, Chen X, Xu X, Gao X. The altered pattern of the functional connectome related to pathological biomarkers in individuals for autism spectrum disorder identification. *Front Neurosci*. 2022;16:913377. doi:10.3389/fnins.2022.913377
146. Hu J, Cao L, Li T, Dong S, Li P. GAT-LI: a graph attention network based learning and interpreting method for functional brain network classification. *BMC Bioinformatics*. 2021;22(1):379. doi:10.1186/s12859-021-04295-1
147. Grossi E, Valbusa G, Buscema M. Detection of an autism EEG signature from only two EEG channels through features extraction and advanced machine learning analysis. *Clin EEG Neurosci*. 2021;52(5):330-337. doi:10.1177/1550059420982424
148. Chen H, Chen W, Song Y, Sun L, Li X. EEG characteristics of children with attention-deficit/hyperactivity disorder. *Neuroscience*. 2019;406:444-456. doi:10.1016/j.neuroscience.2019.03.048

149. Guo X, Yao D, Cao Q, et al. Shared and distinct resting functional connectivity in children and adults with attention-deficit/hyperactivity disorder. *Transl Psychiatry*. 2020;10(1):65. doi:10.1038/s41398-020-0740-y
150. Müller A, Vetsch S, Pershin I, et al. EEG/ERP-based biomarker/neuroalgorithms in adults with ADHD: Development, reliability, and application in clinical practice. *World J Biol Psychiatry*. 2020;21(3):172-182. doi:10.1080/15622975.2019.1605198
151. Gao MS, Tsai FS, Lee CC. Learning a phenotypic-attribute attentional brain connectivity embedding for ADHD classification using rs-fMRI. *Annu Int Conf IEEE Eng Med Biol Soc*. 2020;2020:5472-5475. doi:10.1109/EMBC44109.2020.9175789
152. Chen Y, Tang Y, Wang C, Liu X, Zhao L, Wang Z. ADHD classification by dual subspace learning using resting-state functional connectivity. *Artif Intell Med*. 2020;103:101786. doi:10.1016/j.artmed.2019.101786
153. Muthuraman M, Moliadze V, Boecher L, et al. Multimodal alterations of directed connectivity profiles in patients with attention-deficit/hyperactivity disorders. *Sci Rep*. 2019;9(1):20028. doi:10.1038/s41598-019-56398-8
154. McNorgan C, Judson C, Handzlik D, Holden JG. Linking ADHD and behavioral assessment through identification of shared diagnostic task-based functional connections. *Front Physiol*. 2020;11:583005. doi:10.3389/fphys.2020.583005
155. Vahid A, Bluschke A, Roessner V, Stober S, Beste C. Deep learning based on event-related EEG differentiates children with ADHD from healthy controls. *J Clin Med*. 2019;8(7):1055. doi:10.3390/jcm8071055
156. Riaz A, Asad M, Alonso E, Slabaugh G. DeepfMRI: end-to-end deep learning for functional connectivity and classification of ADHD using fMRI. *J Neurosci Methods*. 2020;335:108506. doi:10.1016/j.jneumeth.2019.108506
157. Rostami M, Farashi S, Khosrowabadi R, Pouretamad H. Discrimination of ADHD subtypes using decision tree on behavioral, neuropsychological, and neural markers. *Basic Clin Neurosci*. 2020;11(3):359-367.
158. Kiiski H, Rueda-Delgado LM, Bennett M, et al. Functional EEG connectivity is a neuromarker for adult attention deficit hyperactivity disorder symptoms. *Clin Neurophysiol*. 2020;131(1):330-342. doi:10.1016/j.clinph.2019.08.010
159. Tang Y, Wang C, Chen Y, Sun N, Jiang A, Wang Z. Identifying ADHD individuals from resting-state functional connectivity using subspace clustering and binary hypothesis testing. *J Atten Disord*. 2021;25(5):736-748. doi:10.1177/1087054719837749
160. Sun Y, Zhao L, Lan Z, Jia XZ, Xue SW. Differentiating boys with ADHD from those with typical development based on whole-brain functional connections using a machine learning approach. *Neuropsychiatr Dis Treat*. 2020;16:691-702. doi:10.2147/NDT.S239013
161. Sidhu G. Locally linear embedding and fMRI feature selection in psychiatric classification. *IEEE J Transl Eng Health Med*. 2019;7:2200211. doi:10.1109/JTEHM.2019.2936348
162. Riaz A, Asad M, Alonso E, Slabaugh G. Fusion of fMRI and non-imaging data for ADHD classification. *Comput Med Imaging Graph*. 2018;65:115-128. doi:10.1016/j.compmedimag.2017.10.002
163. Kaur S, Singh S, Arun P, Kaur D, Bajaj M. Phase space reconstruction of EEG signals for classification of ADHD and control adults. *Clin EEG Neurosci*. 2020;51(2):102-113. doi:10.1177/1550059419876525
164. Chen M, Li H, Wang J, Dillman JR, Parikh NA, He L. A multichannel deep neural network model analyzing multiscale functional brain connectome data for attention deficit hyperactivity disorder detection. *Radiol Artif Intell*. 2019;2(1):e190012. doi:10.1148/ryai.2019190012
165. Sutoko S, Monden Y, Tokuda T, et al. Exploring attentive task-based connectivity for screening attention deficit/hyperactivity disorder children: a functional near-infrared spectroscopy study. *Neurophotonics*. 2019;6(4):045013. doi:10.1117/1.NPh.6.4.045013
166. Luo Y, Alvarez TL, Halperin JM, Li X. Multimodal neuroimaging-based prediction of adult outcomes in childhood-onset ADHD using ensemble learning techniques. *Neuroimage Clin*. 2020;26:102238. doi:10.1016/j.nicl.2020.102238
167. Wang XH, Jiao Y, Li L. Diagnostic model for attention-deficit hyperactivity disorder based on interregional morphological connectivity. *Neurosci Lett*. 2018;685:30-34. doi:10.1016/j.neulet.2018.07.029
168. Peng X, Lin P, Zhang T, Wang J. Extreme learning machine-based classification of ADHD using brain structural MRI data. *PLoS One*. 2013;8(11):e79476. doi:10.1371/journal.pone.0079476
169. Yasumura A, Omori M, Fukuda A, et al. Applied machine learning method to predict children with ADHD using prefrontal cortex activity: a multicenter study in Japan. *J Atten Disord*. 2020;24(14):2012-2020. doi:10.1177/1087054717740632

170. Qureshi MNI, Oh J, Min B, Jo HJ, Lee B. Multi-modal, multi-measure, and multi-class discrimination of ADHD with hierarchical feature extraction and extreme learning machine using structural and functional brain MRI. *Front Hum Neurosci*. 2017;11:157.
171. Biederman J, Hammerness P, Sadeh B, et al. Diagnostic utility of brain activity flow patterns analysis in attention deficit hyperactivity disorder. *Psychol Med*. 2017;47(7):1259-1270. doi:10.1017/S0033291716003329
172. Gehrlicke JG, Kruggel F, Thampipop T, et al. The brain anatomy of attention-deficit/hyperactivity disorder in young adults: a magnetic resonance imaging study. *PLoS One*. 2017;12(4):e0175433. doi:10.1371/journal.pone.0175433
173. Sato JR, Hoexter MQ, Fujita A, Rohde LA. Evaluation of pattern recognition and feature extraction methods in ADHD prediction. *Front Syst Neurosci*. 2012;6:68. doi:10.3389/fnsys.2012.00068
174. Iannaccone R, Hauser TU, Ball J, Brandeis D, Walitza S, Brem S. Classifying adolescent attention-deficit/hyperactivity disorder (ADHD) based on functional and structural imaging. *Eur Child Adolesc Psychiatry*. 2015;24(10):1279-1289. doi:10.1007/s00787-015-0678-4
175. Gu Y, Miao S, Han J, et al. Identifying ADHD children using hemodynamic responses during a working memory task measured by functional near-infrared spectroscopy. *J Neural Eng*. 2018;15(3):035005. doi:10.1088/1741-2552/aa9ee9
176. Du J, Wang L, Jie B, Zhang D. Network-based classification of ADHD patients using discriminative subnetwork selection and graph kernel PCA. *Comput Med Imaging Graph*. 2016;52:82-88. doi:10.1016/j.compmedimag.2016.04.004
177. Wang XH, Jiao Y, Li L. Identifying individuals with attention deficit hyperactivity disorder based on temporal variability of dynamic functional connectivity. *Sci Rep*. 2018;8(1):11789. doi:10.1038/s41598-018-30308-w
178. Hart H, Chantiluke K, Cubillo AI, et al. Pattern classification of response inhibition in ADHD: toward the development of neurobiological markers for ADHD. *Hum Brain Mapp*. 2014;35(7):3083-3094. doi:10.1002/hbm.22386
179. Dai D, Wang J, Hua J, He H. Classification of ADHD children through multimodal magnetic resonance imaging. *Front Syst Neurosci*. 2012;6:63. doi:10.3389/fnsys.2012.00063
180. Liu S, Zhao L, Wang X, et al. Deep spatio-temporal representation and ensemble classification for attention deficit/hyperactivity disorder. *IEEE Trans Neural Syst Rehabil Eng*. 2021;29:1-10. doi:10.1109/TNSRE.2020.3019063
181. Wang X, Jiao Y, Tang T, Wang H, Lu Z. Altered regional homogeneity patterns in adults with attention-deficit hyperactivity disorder. *Eur J Radiol*. 2013;82(9):1552-1557. doi:10.1016/j.ejrad.2013.04.009
182. Sidhu GS, Asgarian N, Greiner R, Brown MR. Kernel principal component analysis for dimensionality reduction in fMRI-based diagnosis of ADHD. *Front Syst Neurosci*. 2012;6:74. doi:10.3389/fnsys.2012.00074
183. Liechti MD, Valko L, Müller UC, et al. Diagnostic value of resting electroencephalogram in attention-deficit/hyperactivity disorder across the lifespan. *Brain Topogr*. 2013;26(1):135-151. doi:10.1007/s10548-012-0258-6
184. Zhu CZ, Zang YF, Cao QJ, et al. Fisher discriminative analysis of resting-state brain function for attention-deficit/hyperactivity disorder. *Neuroimage*. 2008;40(1):110-120. doi:10.1016/j.neuroimage.2007.11.029
185. Olivetti E, Greiner S, Avesani P. ADHD diagnosis from multiple data sources with batch effects. *Front Syst Neurosci*. 2012;6:70. doi:10.3389/fnsys.2012.00070
186. Johnston BA, Mwangi B, Matthews K, Coghill D, Konrad K, Steele JD. Brainstem abnormalities in attention deficit hyperactivity disorder support high accuracy individual diagnostic classification. *Hum Brain Mapp*. 2014;35(10):5179-5189. doi:10.1002/hbm.22542
187. Aradhya AMS, Subbaraju V, Sundaram S, Sundararajan N. Regularized Spatial Filtering Method (R-SFM) for detection of attention deficit hyperactivity disorder (ADHD) from resting-state functional magnetic resonance imaging (rs-fMRI). *Annu Int Conf IEEE Eng Med Biol Soc*. 2018;2018:5541-5544. doi:10.1109/EMBC.2018.8513522
188. Chang CW, Ho CC, Chen JH. ADHD classification by a texture analysis of anatomical brain MRI data. *Front Syst Neurosci*. 2012;6:66. doi:10.3389/fnsys.2012.00066
189. Smith JL, Johnstone SJ, Barry RJ. Aiding diagnosis of attention-deficit/hyperactivity disorder and its subtypes: discriminant function analysis of event-related potential data. *J Child Psychol Psychiatry*. 2003;44(7):1067-1075. doi:10.1111/1469-7610.00191
190. dos Santos Siqueira A, Biazoli Junior CE, Comfort WE, Rohde LA, Sato JR. Abnormal functional resting-state networks in ADHD: graph theory and pattern recognition analysis of fMRI data. *Biomed Res Int*. 2014;2014:380531. doi:10.1155/2014/380531

191. Sun H, Chen Y, Huang Q, et al. Psychoradiologic utility of MR imaging for diagnosis of attention deficit hyperactivity disorder: a radiomics analysis. *Radiology*. 2018;287(2):620-630. doi:10.1148/radiol.2017170226
192. Mueller A, Candrian G, Kropotov JD, Ponomarev VA, Baschera GM. Classification of ADHD patients on the basis of independent ERP components using a machine learning system. *Nonlinear Biomed Phys*. 2010;4(Suppl 1)(suppl 1):S1. doi:10.1186/1753-4631-4-S1-S1
193. Cheng W, Ji X, Zhang J, Feng J. Individual classification of ADHD patients by integrating multiscale neuroimaging markers and advanced pattern recognition techniques. *Front Syst Neurosci*. 2012;6:58. doi:10.3389/fnsys.2012.00058
194. Ahmadlou M, Adeli H. Wavelet-synchronization methodology: a new approach for EEG-based diagnosis of ADHD. *Clin EEG Neurosci*. 2010;41(1):1-10. doi:10.1177/155005941004100103
195. Abibullaev B, An J. Decision support algorithm for diagnosis of ADHD using electroencephalograms. *J Med Syst*. 2012;36(4):2675-2688. doi:10.1007/s10916-011-9742-x
196. Colby JB, Rudie JD, Brown JA, Douglas PK, Cohen MS, Shehzad Z. Insights into multimodal imaging classification of ADHD. *Front Syst Neurosci*. 2012;6:59. doi:10.3389/fnsys.2012.00059
197. Mueller A, Candrian G, Grane VA, Kropotov JD, Ponomarev VA, Baschera GM. Discriminating between ADHD adults and controls using independent ERP components and a support vector machine: a validation study. *Nonlinear Biomed Phys*. 2011;5:5. doi:10.1186/1753-4631-5-5
198. Yu D. Additional brain functional network in adults with attention-deficit/hyperactivity disorder: a phase synchrony analysis. *PLoS One*. 2013;8(1):e54516. doi:10.1371/journal.pone.0054516
199. Poil SS, Bollmann S, Ghisleni C, et al. Age dependent electroencephalographic changes in attention-deficit/hyperactivity disorder (ADHD). *Clin Neurophysiol*. 2014;125(8):1626-1638. doi:10.1016/j.clinph.2013.12.118
200. Qureshi MN, Min B, Jo HJ, Lee B. Multiclass classification for the differential diagnosis on the ADHD subtypes using recursive feature elimination and hierarchical extreme learning machine: structural MRI study. *PLoS One*. 2016;11(8):e0160697. doi:10.1371/journal.pone.0160697
201. Hart H, Marquand AF, Smith A, et al. Predictive neurofunctional markers of attention-deficit/hyperactivity disorder based on pattern classification of temporal processing. *J Am Acad Child Adolesc Psychiatry*. 2014;53(5):569-78.e1. doi:10.1016/j.jaac.2013.12.024
202. Qureshi MNI, Lee B. Classification of ADHD subgroup with recursive feature elimination for structural brain MRI. *Annu Int Conf IEEE Eng Med Biol Soc*. 2016;2016:5929-5932. doi:10.1109/EMBC.2016.7592078
203. Deshpande G, Wang P, Rangaprakash D, Wilamowski B. Fully connected cascade artificial neural network architecture for attention deficit hyperactivity disorder classification from functional magnetic resonance imaging data. *IEEE Trans Cybern*. 2015;45(12):2668-2679. doi:10.1109/TCYB.2014.2379621
204. Hammer R, Cooke GE, Stein MA, Booth JR. Functional neuroimaging of visuospatial working memory tasks enables accurate detection of attention deficit and hyperactivity disorder. *Neuroimage Clin*. 2015;9:244-252. doi:10.1016/j.nicl.2015.08.015
205. Moghaddari M, Lighvan MZ, Danishvar S. Diagnose ADHD disorder in children using convolutional neural network based on continuous mental task EEG. *Comput Methods Programs Biomed*. 2020;197:105738. doi:10.1016/j.cmpb.2020.105738
206. Pereda E, García-Torres M, Melián-Batista B, Mañas S, Méndez L, González JJ. The blessing of dimensionality: feature selection outperforms functional connectivity-based feature transformation to classify ADHD subjects from EEG patterns of phase synchronisation. *PLoS One*. 2018;13(8):e0201660. doi:10.1371/journal.pone.0201660
207. Lim L, Marquand A, Cubillo AA, et al. Disorder-specific predictive classification of adolescents with attention deficit hyperactivity disorder (ADHD) relative to autism using structural magnetic resonance imaging. *PLoS One*. 2013;8(5):e63660. doi:10.1371/journal.pone.0063660
208. Öztoprak H, Toyçan M, Alp YK, Ankan O, Doğutepe E, Karakaş S. Machine-based classification of ADHD and nonADHD participants using time/frequency features of event-related neuroelectric activity. *Clin Neurophysiol*. 2017;128(12):2400-2410. doi:10.1016/j.clinph.2017.09.105
209. Tor HT, Ooi CP, Lim-Ashworth NS, et al. Automated detection of conduct disorder and attention deficit hyperactivity disorder using decomposition and nonlinear techniques with EEG signals. *Comput Methods Programs Biomed*. 2021;200:105941. doi:10.1016/j.cmpb.2021.105941
210. Tosun M. Effects of spectral features of EEG signals recorded with different channels and recording statuses on ADHD classification with deep learning. *Phys Eng Sci Med*. 2021;44(3):693-702. doi:10.1007/s13246-021-01018-x

211. Johnstone SJ, Parrish L, Jiang H, Zhang DW, Williams V, Li S. Aiding diagnosis of childhood attention-deficit/hyperactivity disorder of the inattentive presentation: discriminant function analysis of multi-domain measures including EEG. *Biol Psychol*. 2021;161:108080. doi:10.1016/j.biopsycho.2021.108080
212. Dey S, Rao AR, Shah M. Exploiting the brain's network structure in identifying ADHD subjects. *Front Syst Neurosci*. 2012;6:75. doi:10.3389/fnsys.2012.00075
213. Yoo JH, Kim JI, Kim BN, Jeong B. Exploring characteristic features of attention-deficit/hyperactivity disorder: findings from multi-modal MRI and candidate genetic data. *Brain Imaging Behav*. 2020;14(6):2132-2147. doi:10.1007/s11682-019-00164-x
214. Tenev A, Markovska-Simoska S, Kocarev L, Pop-Jordanov J, Müller A, Candrian G. Machine learning approach for classification of ADHD adults. *Int J Psychophysiol*. 2014;93(1):162-166. doi:10.1016/j.ijpsycho.2013.01.008
215. Rezaeezadeh M, Shamekhi S, Shamsi M. Attention deficit hyperactivity disorder diagnosis using non-linear univariate and multivariate EEG measurements: a preliminary study. *Phys Eng Sci Med*. 2020;43(2):577-592. doi:10.1007/s13246-020-00858-3
216. Crippa A, Salvatore C, Molteni E, et al. The utility of a computerized algorithm based on a multi-domain profile of measures for the diagnosis of attention deficit/hyperactivity disorder. *Front Psychiatry*. 2017;8:189. doi:10.3389/fpsy.2017.00189
217. Ishii-Takahashi A, Takizawa R, Nishimura Y, et al. Prefrontal activation during inhibitory control measured by near-infrared spectroscopy for differentiating between autism spectrum disorders and attention deficit hyperactivity disorder in adults. *Neuroimage Clin*. 2013;4:53-63. doi:10.1016/j.nicl.2013.10.002
218. Zhang T, Li C, Li P, et al. Separated channel attention convolutional neural network (SC-CNN-Attention) to identify ADHD in multi-site Rs-fMRI dataset. *Entropy (Basel)*. 2020;22(8):893. doi:10.3390/e22080893
219. Abramov DM, Lazarev VV, Gomes Junior SC, et al. Estimating biological accuracy of DSM for attention deficit/hyperactivity disorder based on multivariate analysis for small samples. *PeerJ*. 2019;7:e7074. doi:10.7717/peerj.7074
220. Dey S, Rao AR, Shah M. Attributed graph distance measure for automatic detection of attention deficit hyperactive disordered subjects. *Front Neural Circuits*. 2014;8:64. doi:10.3389/fncir.2014.00064
221. Helgadóttir H, Gudmundsson ÓÓ, Baldursson G, et al. Electroencephalography as a clinical tool for diagnosing and monitoring attention deficit hyperactivity disorder: a cross-sectional study. *BMJ Open*. 2015;5(1):e005500. doi:10.1136/bmjopen-2014-005500
222. Chow JC, Ouyang CS, Tsai CL, et al. Entropy-based quantitative electroencephalogram analysis for diagnosing attention-deficit hyperactivity disorder in girls. *Clin EEG Neurosci*. 2019;50(3):172-179. doi:10.1177/1550059418814983
223. Chen H, Song Y, Li X. Use of deep learning to detect personalized spatial-frequency abnormalities in EEGs of children with ADHD. *J Neural Eng*. 2019;16(6):066046. doi:10.1088/1741-2552/ab3a0a
224. Jahanshahloo HR, Shamsi M, Ghasemi E, Kouhi A. Automated and ERP-based diagnosis of attention-deficit hyperactivity disorder in children. *J Med Signals Sens*. 2017;7(1):26-32. doi:10.4103/2228-7477.199152
225. Wolfers T, van Rooij D, Oosterlaan J, et al. Quantifying patterns of brain activity: distinguishing unaffected siblings from participants with ADHD and healthy individuals. *Neuroimage Clin*. 2016;12:227-233. doi:10.1016/j.nicl.2016.06.020
226. Shao L, You Y, Du H, Fu D. Classification of ADHD with fMRI data and multi-objective optimization. *Comput Methods Programs Biomed*. 2020;196:105676. doi:10.1016/j.cmpb.2020.105676
227. Itani S, Rossignol M, Lecron F, Fortemps P. Towards interpretable machine learning models for diagnosis aid: a case study on attention deficit/hyperactivity disorder. *PLoS One*. 2019;14(4):e0215720. doi:10.1371/journal.pone.0215720
228. Khoshnoud S, Nazari MA, Shamsi M. Functional brain dynamic analysis of ADHD and control children using nonlinear dynamical features of EEG signals. *J Integr Neurosci*. 2018;17(1):11-17. doi:10.3233/JIN-170033
229. Chikara RK, Ko LW. Neural activities classification of human inhibitory control using hierarchical model. *Sensors (Basel)*. 2019;19(17):3791. doi:10.3390/s19173791
230. Zhou X, Lin Q, Gui Y, Wang Z, Liu M, Lu H. Multimodal MR images-based diagnosis of early adolescent attention-deficit/hyperactivity disorder using multiple kernel learning. *Front Neurosci*. 2021;15:710133. doi:10.3389/fnins.2021.710133
231. Zhou D, Liao Z, Chen R. Deep learning enabled diagnosis of children's ADHD based on the big data of video screen long-range EEG. *J Healthc Eng*. 2022;2022:5222136. doi:10.1155/2022/5222136

232. Tang Y, Sun J, Wang C, et al. ADHD classification using auto-encoding neural network and binary hypothesis testing. *Artif Intell Med*. 2022;123:102209. doi:10.1016/j.artmed.2021.102209
233. Catherine Joy R, Thomas George S, Albert Rajan A, Subathra MSP. Detection of ADHD from EEG signals using different entropy measures and ANN. *Clin EEG Neurosci*. 2022;53(1):12-23. doi:10.1177/15500594211036788
234. Zhao K, Duka B, Xie H, Oathes DJ, Calhoun V, Zhang Y. A dynamic graph convolutional neural network framework reveals new insights into connectome dysfunctions in ADHD. *Neuroimage*. 2022;246:118774. doi:10.1016/j.neuroimage.2021.118774
235. Wang Z, Zhu Y, Shi H, Zhang Y, Yan C. A 3D multiscale view convolutional neural network with attention for mental disease diagnosis on MRI images. *Math Biosci Eng*. 2021;18(5):6978-6994. doi:10.3934/mbe.2021347
236. Dinkel PJ, Willmes K, Krinzing H, Konrad K, Koten JW Jr. Diagnosing developmental dyscalculia on the basis of reliable single case fMRI methods: promises and limitations. *PLoS One*. 2013;8(12):e83722. doi:10.1371/journal.pone.0083722
237. Zahia S, Garcia-Zapirain B, Saralegui I, Fernandez-Ruanova B. Dyslexia detection using 3D convolutional neural networks and functional magnetic resonance imaging. *Comput Methods Programs Biomed*. 2020;197:105726. doi:10.1016/j.cmpb.2020.105726
238. Płoński P, Gradkowski W, Altarelli I, et al. Multi-parameter machine learning approach to the neuroanatomical basis of developmental dyslexia. *Hum Brain Mapp*. 2017;38(2):900-908. doi:10.1002/hbm.23426
239. Martinez-Murcia FJ, Ortiz A, Gorriz JM, et al. EEG connectivity analysis using denoising autoencoders for the detection of dyslexia. *Int J Neural Syst*. 2020;30(7):2050037. doi:10.1142/S0129065720500379
240. Zainuddin AZA, Mansor W, Lee KY, Mahmoodin Z. Comparison of extreme learning machine and K-nearest neighbour performance in classifying EEG signal of normal, poor and capable dyslexic children. *Annu Int Conf IEEE Eng Med Biol Soc*. 2019;2019:4513-4516. doi:10.1109/EMBC.2019.8857569
241. Serrallach B, Groß C, Bernhofs V, et al. Neural biomarkers for dyslexia, ADHD, and ADD in the auditory cortex of children. *Front Neurosci*. 2016;10:324. doi:10.3389/fnins.2016.00324
242. Cui Z, Xia Z, Su M, Shu H, Gong G. Disrupted white matter connectivity underlying developmental dyslexia: a machine learning approach. *Hum Brain Mapp*. 2016;37(4):1443-1458. doi:10.1002/hbm.23112
243. García-Chimeno Y, García-Zapirain B, Saralegui Prieto I, Fernandez-Ruanova B. Automatic classification of dyslexic children by applying machine learning to fMRI images. *Biomed Mater Eng*. 2014;24(6):2995-3002. doi:10.3233/BME-141120
244. Bailey S, Hoeff F, Aboud K, Cutting L. Anomalous gray matter patterns in specific reading comprehension deficit are independent of dyslexia. *Ann Dyslexia*. 2016;66(3):256-274. doi:10.1007/s11881-015-0114-y
245. Usman OL, Muniyandi RC, Omar K, Mohamad M. Gaussian smoothing and modified histogram normalization methods to improve neural-biomarker interpretations for dyslexia classification mechanism. *PLoS One*. 2021;16(2):e0245579. doi:10.1371/journal.pone.0245579
246. Mascheretti S, Peruzzo D, Andreola C, et al. Selecting the most relevant brain regions to classify children with developmental dyslexia and typical readers by using complex magnocellular stimuli and multiple kernel learning. *Brain Sci*. 2021;11(6):722. doi:10.3390/brainsci11060722
247. Li A, Zalesky A, Yue W, et al. A neuroimaging biomarker for striatal dysfunction in schizophrenia. *Nat Med*. 2020;26(4):558-565. doi:10.1038/s41591-020-0793-8
248. Jo YT, Joo SW, Shon SH, Kim H, Kim Y, Lee J. Diagnosing schizophrenia with network analysis and a machine learning method. *Int J Methods Psychiatr Res*. 2020;29(1):e1818. doi:10.1002/mpr.1818
249. Yassin W, Nakatani H, Zhu Y, et al. Machine-learning classification using neuroimaging data in schizophrenia, autism, ultra-high risk and first-episode psychosis. *Transl Psychiatry*. 2020;10(1):278. doi:10.1038/s41398-020-00965-5
250. Chen Z, Yan T, Wang E, et al. Detecting abnormal brain regions in schizophrenia using structural MRI via machine learning. *Comput Intell Neurosci*. 2020;2020:6405930. doi:10.1155/2020/6405930
251. Jahmunah V, Lih Oh S, Rajinikanth V, et al. Automated detection of schizophrenia using nonlinear signal processing methods. *Artif Intell Med*. 2019;100:101698. doi:10.1016/j.artmed.2019.07.006
252. Wang L, Li X, Zhu Y, et al. Discriminative analysis of symptom severity and ultra-high risk of schizophrenia using intrinsic functional connectivity. *Int J Neural Syst*. 2020;30(9):2050047. doi:10.1142/S0129065720500471
253. Mikolas P, Hlinka J, Skoch A, et al. Machine learning classification of first-episode schizophrenia spectrum disorders and controls using whole brain white matter fractional anisotropy. *BMC Psychiatry*. 2018;18(1):97. doi:10.1186/s12888-018-1678-y

254. Schwarz E, Doan NT, Pergola G, et al; IMAGEMEND Consortium, Karolinska Schizophrenia Project (KaSP) Consortium. Reproducible grey matter patterns index a multivariate, global alteration of brain structure in schizophrenia and bipolar disorder. *Transl Psychiatry*. 2019;9(1):12. doi:10.1038/s41398-018-0225-4
255. Baradits M, Bitter I, Czobor P. Multivariate patterns of EEG microstate parameters and their role in the discrimination of patients with schizophrenia from healthy controls. *Psychiatry Res*. 2020;288:112938. doi:10.1016/j.psychres.2020.112938
256. Kim J, Kim MY, Kwon H, et al. Feature optimization method for machine learning-based diagnosis of schizophrenia using magnetoencephalography. *J Neurosci Methods*. 2020;338:108688. doi:10.1016/j.jneumeth.2020.108688
257. de Moura AM, Pinaya WHL, Gadelha A, et al. Investigating brain structural patterns in first episode psychosis and schizophrenia using MRI and a machine learning approach. *Psychiatry Res Neuroimaging*. 2018;275:14-20. doi:10.1016/j.pscychresns.2018.03.003
258. Yamamoto M, Bagarinao E, Kushima I, et al. Support vector machine-based classification of schizophrenia patients and healthy controls using structural magnetic resonance imaging from two independent sites. *PLoS One*. 2020;15(11):e0239615. doi:10.1371/journal.pone.0239615
259. Zou H, Yang J. Dynamic thresholding networks for schizophrenia diagnosis. *Artif Intell Med*. 2019;96:25-32. doi:10.1016/j.artmed.2019.03.007
260. Rozycki M, Satterthwaite TD, Koutsouleris N, et al. Multisite machine learning analysis provides a robust structural imaging signature of schizophrenia detectable across diverse patient populations and within individuals. *Schizophr Bull*. 2018;44(5):1035-1044. doi:10.1093/schbul/sbx137
261. Liang S, Deng W, Li X, et al. Aberrant posterior cingulate connectivity classify first-episode schizophrenia from controls: a machine learning study. *Schizophr Res*. 2020;220:187-193. doi:10.1016/j.schres.2020.03.022
262. Alamian G, Pascarella A, Lajnef T, et al. Patient, interrupted: MEG oscillation dynamics reveal temporal dysconnectivity in schizophrenia. *Neuroimage Clin*. 2020;28:102485. doi:10.1016/j.nicl.2020.102485
263. de Pierrefeu A, Löfstedt T, Laidi C, et al. Identifying a neuroanatomical signature of schizophrenia, reproducible across sites and stages, using machine learning with structured sparsity. *Acta Psychiatr Scand*. 2018;138(6):571-580. doi:10.1111/acps.12964
264. Di Carlo P, Pergola G, Antonucci LA, et al. Multivariate patterns of gray matter volume in thalamic nuclei are associated with positive schizotypy in healthy individuals. *Psychol Med*. 2020;50(9):1501-1509. doi:10.1017/S0033291719001430
265. Bae Y, Kumarasamy K, Ali IM, Korfiatis P, Akkus Z, Erickson BJ. Differences between schizophrenic and normal subjects using network properties from fMRI. *J Digit Imaging*. 2018;31(2):252-261. doi:10.1007/s10278-017-0020-4
266. Yu Y, Shen H, Zeng LL, Ma Q, Hu D. Convergent and divergent functional connectivity patterns in schizophrenia and depression. *PLoS One*. 2013;8(7):e68250. doi:10.1371/journal.pone.0068250
267. Dluhoš P, Schwarz D, Cahn W, et al. Multi-center machine learning in imaging psychiatry: a meta-model approach. *Neuroimage*. 2017;155:10-24. doi:10.1016/j.neuroimage.2017.03.027
268. Lee J, Chon MW, Kim H, et al. Diagnostic value of structural and diffusion imaging measures in schizophrenia. *Neuroimage Clin*. 2018;18:467-474. doi:10.1016/j.nicl.2018.02.007
269. Antonucci LA, Penzel N, Pergola G, et al. Multivariate classification of schizophrenia and its familial risk based on load-dependent attentional control brain functional connectivity. *Neuropsychopharmacology*. 2020;45(4):613-621. doi:10.1038/s41386-019-0532-3
270. Lu X, Yang Y, Wu F, et al. Discriminative analysis of schizophrenia using support vector machine and recursive feature elimination on structural MRI images. *Medicine (Baltimore)*. 2016;95(30):e3973. doi:10.1097/MD.0000000000003973
271. Chyzyk D, Graña M, Öngür D, Shinn AK. Discrimination of schizophrenia auditory hallucinators by machine learning of resting-state functional MRI. *Int J Neural Syst*. 2015;25(3):1550007. doi:10.1142/S0129065715500070
272. Jing R, Li P, Ding Z, et al. Machine learning identifies unaffected first-degree relatives with functional network patterns and cognitive impairment similar to those of schizophrenia patients. *Hum Brain Mapp*. 2019;40(13):3930-3939. doi:10.1002/hbm.24678
273. Hua M, Peng Y, Zhou Y, Qin W, Yu C, Liang M. Disrupted pathways from limbic areas to thalamus in schizophrenia highlighted by whole-brain resting-state effective connectivity analysis. *Prog Neuropsychopharmacol Biol Psychiatry*. 2020;99:109837. doi:10.1016/j.pnpbp.2019.109837

274. Gould IC, Shepherd AM, Laurens KR, Cairns MJ, Carr VJ, Green MJ. Multivariate neuroanatomical classification of cognitive subtypes in schizophrenia: a support vector machine learning approach. *Neuroimage Clin*. 2014;6:229-236. doi:10.1016/j.nicl.2014.09.009
275. Song H, Chen L, Gao R, et al. Automatic schizophrenic discrimination on fNIRS by using complex brain network analysis and SVM. *BMC Med Inform Decis Mak*. 2017;17(suppl 3):166. doi:10.1186/s12911-017-0559-5
276. Zhu Q, Huang J, Xu X. Non-negative discriminative brain functional connectivity for identifying schizophrenia on resting-state fMRI. *Biomed Eng Online*. 2018;17(1):32. doi:10.1186/s12938-018-0464-x
277. Zhao W, Guo S, Linli Z, Yang AC, Lin CP, Tsai SJ. Functional, anatomical, and morphological networks highlight the role of basal ganglia-thalamus-cortex circuits in schizophrenia. *Schizophr Bull*. 2020;46(2):422-431.
278. Chin R, You AX, Meng F, Zhou J, Sim K. Recognition of schizophrenia with regularized support vector machine and sequential region of interest selection using structural magnetic resonance imaging. *Sci Rep*. 2018;8(1):13858. doi:10.1038/s41598-018-32290-9
279. Iwabuchi SJ, Palaniyappan L. Abnormalities in the effective connectivity of visuothalamic circuitry in schizophrenia. *Psychol Med*. 2017;47(7):1300-1310. doi:10.1017/S0033291716003469
280. Winterburn JL, Voineskos AN, Devenyi GA, et al. Can we accurately classify schizophrenia patients from healthy controls using magnetic resonance imaging and machine learning? a multi-method and multi-dataset study. *Schizophr Res*. 2019;214:3-10. doi:10.1016/j.schres.2017.11.038
281. Chen H, Uddin LQ, Duan X, et al. Shared atypical default mode and salience network functional connectivity between autism and schizophrenia. *Autism Res*. 2017;10(11):1776-1786. doi:10.1002/aur.1834
282. Xiao Y, Yan Z, Zhao Y, et al. Support vector machine-based classification of first episode drug-naïve schizophrenia patients and healthy controls using structural MRI. *Schizophr Res*. 2019;214:11-17. doi:10.1016/j.schres.2017.11.037
283. Zeng LL, Wang H, Hu P, et al. Multi-site diagnostic classification of schizophrenia using discriminant deep learning with functional connectivity MRI. *EBioMedicine*. 2018;30:74-85. doi:10.1016/j.ebiom.2018.03.017
284. Supekar K, Cai W, Krishnadas R, Palaniyappan L, Menon V. Dysregulated brain dynamics in a triple-network saliency model of schizophrenia and its relation to psychosis. *Biol Psychiatry*. 2019;85(1):60-69. doi:10.1016/j.biopsych.2018.07.020
285. Mastrovito D, Hanson C, Hanson SJ. Differences in atypical resting-state effective connectivity distinguish autism from schizophrenia. *Neuroimage Clin*. 2018;18:367-376. doi:10.1016/j.nicl.2018.01.014
286. Liu Y, Zhang Y, Lv L, Wu R, Zhao J, Guo W. Abnormal neural activity as a potential biomarker for drug-naïve first-episode adolescent-onset schizophrenia with coherence regional homogeneity and support vector machine analyses. *Schizophr Res*. 2018;192:408-415. doi:10.1016/j.schres.2017.04.028
287. Cui LB, Liu L, Wang HN, et al. Disease definition for schizophrenia by functional connectivity using radiomics strategy. *Schizophr Bull*. 2018;44(5):1053-1059. doi:10.1093/schbul/sby007
288. Pinaya WHL, Mechelli A, Sato JR. Using deep autoencoders to identify abnormal brain structural patterns in neuropsychiatric disorders: a large-scale multi-sample study. *Hum Brain Mapp*. 2019;40(3):944-954. doi:10.1002/hbm.24423
289. Chen X, Liu C, He H, et al. Transdiagnostic differences in the resting-state functional connectivity of the prefrontal cortex in depression and schizophrenia. *J Affect Disord*. 2017;217:118-124. doi:10.1016/j.jad.2017.04.001
290. Schnack HG, Nieuwenhuis M, van Haren NE, et al. Can structural MRI aid in clinical classification? a machine learning study in two independent samples of patients with schizophrenia, bipolar disorder and healthy subjects. *Neuroimage*. 2014;84:299-306. doi:10.1016/j.neuroimage.2013.08.053
291. Cheng H, Newman S, Goñi J, et al. Nodal centrality of functional network in the differentiation of schizophrenia. *Schizophr Res*. 2015;168(1-2):345-352. doi:10.1016/j.schres.2015.08.011
292. Mikolas P, Melicher T, Skoch A, et al. Connectivity of the anterior insula differentiates participants with first-episode schizophrenia spectrum disorders from controls: a machine-learning study. *Psychol Med*. 2016;46(13):2695-2704. doi:10.1017/S0033291716000878
293. Venkataraman A, Whitford TJ, Westin CF, Golland P, Kubicki M. Whole brain resting state functional connectivity abnormalities in schizophrenia. *Schizophr Res*. 2012;139(1-3):7-12. doi:10.1016/j.schres.2012.04.021
294. Wang S, Zhang Y, Lv L, et al. Abnormal regional homogeneity as a potential imaging biomarker for adolescent-onset schizophrenia: a resting-state fMRI study and support vector machine analysis. *Schizophr Res*. 2018;192:179-184. doi:10.1016/j.schres.2017.05.038

295. Cabral C, Kambeitz-Illankovic L, Kambeitz J, et al. Classifying schizophrenia using multimodal multivariate pattern recognition analysis: evaluating the impact of individual clinical profiles on the neurodiagnostic performance. *Schizophr Bull*. 2016;42(Suppl 1)(suppl 1):S110-S117. doi:10.1093/schbul/sbw053
296. Ebdrup BH, Axelsen MC, Bak N, et al. Accuracy of diagnostic classification algorithms using cognitive-, electrophysiological-, and neuroanatomical data in antipsychotic-naive schizophrenia patients. *Psychol Med*. 2019;49(16):2754-2763. doi:10.1017/S0033291718003781
297. Pinaya WH, Gadelha A, Doyle OM, et al. Using deep belief network modelling to characterize differences in brain morphometry in schizophrenia. *Sci Rep*. 2016;6:38897. doi:10.1038/srep38897
298. Kim J, Calhoun VD, Shim E, Lee JH. Deep neural network with weight sparsity control and pre-training extracts hierarchical features and enhances classification performance: Evidence from whole-brain resting-state functional connectivity patterns of schizophrenia. *Neuroimage*. 2016;124(Pt A):127-146. doi:10.1016/j.neuroimage.2015.05.018
299. Viviano JD, Buchanan RW, Calarco N, et al; Social Processes Initiative in Neurobiology of the Schizophrenia(s) Group. Resting-state connectivity biomarkers of cognitive performance and social function in individuals with schizophrenia spectrum disorder and healthy control subjects. *Biol Psychiatry*. 2018;84(9):665-674. doi:10.1016/j.biopsych.2018.03.013
300. Arbabshirani MR, Castro E, Calhoun VD. Accurate classification of schizophrenia patients based on novel resting-state fMRI features. *Annu Int Conf IEEE Eng Med Biol Soc*. 2014;2014:6691-6694. doi:10.1109/EMBC.2014.6945163
301. Yan W, Calhoun V, Song M, et al. Discriminating schizophrenia using recurrent neural network applied on time courses of multi-site fMRI data. *EBioMedicine*. 2019;47:543-552. doi:10.1016/j.ebiom.2019.08.023
302. Orban P, Dansereau C, Desbois L, et al. Multisite generalizability of schizophrenia diagnosis classification based on functional brain connectivity. *Schizophr Res*. 2018;192:167-171. doi:10.1016/j.schres.2017.05.027
303. Yu Y, Shen H, Zhang H, Zeng LL, Xue Z, Hu D. Functional connectivity-based signatures of schizophrenia revealed by multiclass pattern analysis of resting-state fMRI from schizophrenic patients and their healthy siblings. *Biomed Eng Online*. 2013;12:10. doi:10.1186/1475-925X-12-10
304. Dillon K, Calhoun V, Wang YP. A robust sparse-modeling framework for estimating schizophrenia biomarkers from fMRI. *J Neurosci Methods*. 2017;276:46-55. doi:10.1016/j.jneumeth.2016.11.005
305. Pergola G, Trizio S, Di Carlo P, et al. Grey matter volume patterns in thalamic nuclei are associated with familial risk for schizophrenia. *Schizophr Res*. 2017;180:13-20. doi:10.1016/j.schres.2016.07.005
306. Shen H, Wang L, Liu Y, Hu D. Discriminative analysis of resting-state functional connectivity patterns of schizophrenia using low dimensional embedding of fMRI. *Neuroimage*. 2010;49(4):3110-3121. doi:10.1016/j.neuroimage.2009.11.011
307. Chu WL, Huang MW, Jian BL, Hsu CY, Cheng KS. A correlative classification study of schizophrenic patients with results of clinical evaluation and structural magnetic resonance images. *Behav Neurol*. 2016;2016:7849526. doi:10.1155/2016/7849526
308. Masychev K, Ciprian C, Ravan M, Reilly JP, MacCrimmon D. Advanced signal processing methods for characterization of schizophrenia. *IEEE Trans Biomed Eng*. 2021;68(4):1123-1130. doi:10.1109/TBME.2020.3011842
309. Korda AI, Ruef A, Neufang S, et al. Identification of voxel-based texture abnormalities as new biomarkers for schizophrenia and major depressive patients using layer-wise relevance propagation on deep learning decisions. *Psychiatry Res Neuroimaging*. 2021;313:111303. doi:10.1016/j.pscychresns.2021.111303
310. Pina-Camacho L, Garcia-Prieto J, Parellada M, et al. Predictors of schizophrenia spectrum disorders in early-onset first episodes of psychosis: a support vector machine model. *Eur Child Adolesc Psychiatry*. 2015;24(4):427-440. doi:10.1007/s00787-014-0593-0
311. Castro E, Martínez-Ramón M, Pearson G, Sui J, Calhoun VD. Characterization of groups using composite kernels and multi-source fMRI analysis data: application to schizophrenia. *Neuroimage*. 2011;58(2):526-536. doi:10.1016/j.neuroimage.2011.06.044
312. Koch SP, Hägele C, Haynes JD, Heinz A, Schlagenhaut F, Sterzer P. Diagnostic classification of schizophrenia patients on the basis of regional reward-related fMRI signal patterns. *PLoS One*. 2015;10(3):e0119089. doi:10.1371/journal.pone.0119089
313. Castro E, Gupta CN, Martínez-Ramón M, Calhoun VD, Arbabshirani MR, Turner J. Identification of patterns of gray matter abnormalities in schizophrenia using source-based morphometry and bagging. *Annu Int Conf IEEE Eng Med Biol Soc*. 2014;2014:1513-1516. doi:10.1109/EMBC.2014.6943889

314. Arribas JI, Calhoun VD, Adali T. Automatic bayesian classification of healthy controls, bipolar disorder, and schizophrenia using intrinsic connectivity maps from fMRI data. *IEEE Trans Biomed Eng*. 2010;57(12):2850-2860. doi:10.1109/TBME.2010.2080679
315. Yoon JH, Nguyen DV, McVay LM, et al. Automated classification of fMRI during cognitive control identifies more severely disorganized subjects with schizophrenia. *Schizophr Res*. 2012;135(1-3):28-33. doi:10.1016/j.schres.2012.01.001
316. Chyzyhyk D, Savio A, Graña M. Computer aided diagnosis of schizophrenia on resting state fMRI data by ensembles of ELM. *Neural Netw*. 2015;68:23-33. doi:10.1016/j.neunet.2015.04.002
317. Wang P, Verma R. On classifying disease-induced patterns in the brain using diffusion tensor images. In: Metaxas D, Axel L, Fichtinger G, Székely G., eds. *Medical Image Computing and Computer-Assisted Intervention—MICCAI 2008*. MICCAI 2008. Lecture Notes in Computer Science. Vol 5241. Springer; 2008:908-916.
318. Ince NF, Goksu F, Pellizzer G, Tewfik A, Stephane M. Selection of spectro-temporal patterns in multichannel MEG with support vector machines for schizophrenia classification. *Annu Int Conf IEEE Eng Med Biol Soc*. 2008; 2008:3554-3557. doi:10.1109/IEMBS.2008.4649973
319. Sveinsson JR, Benediktsson JA, Stefansson SB, Davidsson K. Parallel principal component neural networks for classification of event-related potential waveforms. *Med Eng Phys*. 1997;19(1):15-20. doi:10.1016/S1350-4533(96)00035-5
320. Calhas D, Romero E, Henriques R. On the use of pairwise distance learning for brain signal classification with limited observations. *Artif Intell Med*. 2020;105:101852. doi:10.1016/j.artmed.2020.101852
321. Calhoun VD, Maciejewski PK, Pearson GD, Kiehl KA. Temporal lobe and "default" hemodynamic brain modes discriminate between schizophrenia and bipolar disorder. *Hum Brain Mapp*. 2008;29(11):1265-1275. doi:10.1002/hbm.20463
322. Neuhaus AH, Popescu FC, Bates JA, Goldberg TE, Malhotra AK. Single-subject classification of schizophrenia using event-related potentials obtained during auditory and visual oddball paradigms. *Eur Arch Psychiatry Clin Neurosci*. 2013;263(3):241-247. doi:10.1007/s00406-012-0326-7
323. Xu T, Stephane M, Parhi KK. Abnormal neural oscillations in schizophrenia assessed by spectral power ratio of MEG during word processing. *IEEE Trans Neural Syst Rehabil Eng*. 2016;24(11):1148-1158. doi:10.1109/TNSRE.2016.2551700
324. Ravan M, MacCrimmon D, Hasey G, Reilly JP, Khodayari-Rostamabad A. A machine learning approach using P300 responses to investigate effect of clozapine therapy. *Annu Int Conf IEEE Eng Med Biol Soc*. 2012;2012: 5911-5914. doi:10.1109/EMBC.2012.6347339
325. Castellani U, Rossato E, Murino V, et al. Classification of schizophrenia using feature-based morphometry. *J Neural Transm (Vienna)*. 2012;119(3):395-404. doi:10.1007/s00702-011-0693-7
326. Khare S, Bajaj V, Siuly S, Sinha PG. Classification of schizophrenia patients through empirical wavelet transformation using electroencephalogram signals. In: Bajaj V, Sinha GR, eds. *Modelling and Analysis of Active Biopotential Signals in Healthcare, Volume 1*. IOP Publishing Ltd; 2020:1-26.
327. Yan W, Zhao M, Fu Z, Pearson GD, Sui J, Calhoun VD. Mapping relationships among schizophrenia, bipolar and schizoaffective disorders: a deep classification and clustering framework using fMRI time series. *Schizophr Res*. 2022;245:141-150. doi:10.1016/j.schres.2021.02.007
328. Du Y, Hao H, Wang S, Pearson GD, Calhoun VD. Identifying commonality and specificity across psychosis sub-groups via classification based on features from dynamic connectivity analysis. *Neuroimage Clin*. 2020;27: 102284. doi:10.1016/j.nicl.2020.102284
329. Oh K, Kim W, Shen G, et al. Classification of schizophrenia and normal controls using 3D convolutional neural network and outcome visualization. *Schizophr Res*. 2019;212:186-195. doi:10.1016/j.schres.2019.07.034
330. Guo Y, Qiu J, Lu W. Support vector machine-based schizophrenia classification using morphological information from amygdaloid and hippocampal subregions. *Brain Sci*. 2020;10(8):562. doi:10.3390/brainsci10080562
331. Qureshi MNI, Oh J, Cho D, Jo HJ, Lee B. Multimodal discrimination of schizophrenia using hybrid weighted feature concatenation of brain functional connectivity and anatomical features with an extreme learning machine. *Front Neuroinform*. 2017;11:59. doi:10.3389/fninf.2017.00059
332. Gallos IK, Gkiatis K, Matsopoulos GK, Siettos C. ISOMAP and machine learning algorithms for the construction of embedded functional connectivity networks of anatomically separated brain regions from resting state fMRI data of patients with schizophrenia. *AIMS Neurosci*. 2021;8(2):295-321. doi:10.3934/Neuroscience.2021016
333. Wang T, Bezerianos A, Cichocki A, Li J. Multikernel capsule network for schizophrenia identification. *IEEE Trans Cybern*. 2022;52(6):4741-4750. doi:10.1109/TCYB.2020.3035282

334. Zang J, Huang Y, Kong L, et al. Effects of brain atlases and machine learning methods on the discrimination of schizophrenia patients: a multimodal MRI study. *Front Neurosci*. 2021;15:697168. doi:10.3389/fnins.2021.697168
335. Hu M, Qian X, Liu S, et al. Structural and diffusion MRI based schizophrenia classification using 2D pretrained and 3D naive convolutional neural networks. *Schizophr Res*. 2022;243:330-341. doi:10.1016/j.schres.2021.06.011
336. Kim K, Duc NT, Choi M, Lee B. EEG microstate features for schizophrenia classification. *PLoS One*. 2021;16(5):e0251842. doi:10.1371/journal.pone.0251842
337. Salvador R, Canales-Rodríguez E, Guerrero-Pedraza A, et al. Multimodal integration of brain images for MRI-based diagnosis in schizophrenia. *Front Neurosci*. 2019;13:1203. doi:10.3389/fnins.2019.01203
338. Chou PH, Yao YH, Zheng RX, et al. Deep neural network to differentiate brain activity between patients with first-episode schizophrenia and healthy individuals: a multi-channel near infrared spectroscopy study. *Front Psychiatry*. 2021;12:655292. doi:10.3389/fpsyt.2021.655292
339. Li Z, Li W, Wei Y, et al. Deep learning based automatic diagnosis of first-episode psychosis, bipolar disorder and healthy controls. *Comput Med Imaging Graph*. 2021;89:101882. doi:10.1016/j.compmedimag.2021.101882
340. Yang H, Liu J, Sui J, Pearlson G, Calhoun VD. A hybrid machine learning method for fusing fMRI and genetic data: combining both improves classification of schizophrenia. *Front Hum Neurosci*. 2010;4:192. doi:10.3389/fnhum.2010.00192
341. Kalmady SV, Greiner R, Agrawal R, et al. Towards artificial intelligence in mental health by improving schizophrenia prediction with multiple brain parcellation ensemble-learning. *NPJ Schizophr*. 2019;5(1):2. doi:10.1038/s41537-018-0070-8
342. Liu W, Zhang X, Qiao Y, et al. Functional connectivity combined with a machine learning algorithm can classify high-risk first-degree relatives of patients with schizophrenia and identify correlates of cognitive impairments. *Front Neurosci*. 2020;14:577568. doi:10.3389/fnins.2020.577568
343. Bansal R, Staib LH, Laine AF, et al. Anatomical brain images alone can accurately diagnose chronic neuropsychiatric illnesses. *PLoS One*. 2012;7(12):e50698. doi:10.1371/journal.pone.0050698
344. Li F, Wang J, Liao Y, et al. Differentiation of schizophrenia by combining the spatial EEG brain network patterns of rest and task P300. *IEEE Trans Neural Syst Rehabil Eng*. 2019;27(4):594-602. doi:10.1109/TNSRE.2019.2900725
345. Zhao Z, Li J, Niu Y, et al. Classification of schizophrenia by combination of brain effective and functional connectivity. *Front Neurosci*. 2021;15:651439. doi:10.3389/fnins.2021.651439
346. Park SM, Jeong B, Oh DY, et al. Identification of major psychiatric disorders from resting-state electroencephalography using a machine learning approach. *Front Psychiatry*. 2021;12:707581. doi:10.3389/fpsyt.2021.707581
347. Lei D, Pinaya WHL, Young J, et al. Integrating machine learning and multimodal neuroimaging to detect schizophrenia at the level of the individual. *Hum Brain Mapp*. 2020;41(5):1119-1135. doi:10.1002/hbm.24863
348. Kim JY, Lee HS, Lee SH. EEG source network for the diagnosis of schizophrenia and the identification of subtypes based on symptom severity—a machine learning approach. *J Clin Med*. 2020;9(12):3934. doi:10.3390/jcm9123934
349. Shi D, Li Y, Zhang H, et al. Machine learning of schizophrenia detection with structural and functional neuroimaging. *Dis Markers*. 2021;2021:9963824. doi:10.1155/2021/9963824
350. Shalhaf A, Bagherzadeh S, Maghsoudi A. Transfer learning with deep convolutional neural network for automated detection of schizophrenia from EEG signals. *Phys Eng Sci Med*. 2020;43(4):1229-1239. doi:10.1007/s13246-020-00925-9
351. Janousova E, Montana G, Kasperek T, Schwarz D. Supervised, multivariate, whole-brain reduction did not help to achieve high classification performance in schizophrenia research. *Front Neurosci*. 2016;10:392. doi:10.3389/fnins.2016.00392
352. Lieslehto J, Jääskeläinen E, Kiviniemi V, et al. The progression of disorder-specific brain pattern expression in schizophrenia over 9 years. *NPJ Schizophr*. 2021;7(1):32. doi:10.1038/s41537-021-00157-0
353. Ke PF, Xiong DS, Li JH, et al. An integrated machine learning framework for a discriminative analysis of schizophrenia using multi-biological data. *Sci Rep*. 2021;11(1):14636. doi:10.1038/s41598-021-94007-9
354. Gheiratmand M, Rish I, Cecchi GA, et al. Learning stable and predictive network-based patterns of schizophrenia and its clinical symptoms. *NPJ Schizophr*. 2017;3:22. doi:10.1038/s41537-017-0022-8
355. Chen J, Li X, Calhoun VD, et al. Sparse deep neural networks on imaging genetics for schizophrenia case-control classification. *Hum Brain Mapp*. 2021;42(8):2556-2568. doi:10.1002/hbm.25387

356. Oh J, Oh BL, Lee KU, Chae JH, Yun K. Identifying schizophrenia using structural MRI with a deep learning algorithm. *Front Psychiatry*. 2020;11:16. doi:10.3389/fpsy.2020.00016
357. Singh K, Singh S, Malhotra J. Spectral features based convolutional neural network for accurate and prompt identification of schizophrenic patients. *Proc Inst Mech Eng H*. 2021;235(2):167-184. doi:10.1177/0954411920966937
358. Sun J, Cao R, Zhou M, et al. A hybrid deep neural network for classification of schizophrenia using EEG data. *Sci Rep*. 2021;11(1):4706. doi:10.1038/s41598-021-83350-6
359. Li YJ, Fan FY. Classification of schizophrenia and depression by EEG with ANNs*. *Conf Proc IEEE Eng Med Biol Soc*. 2005;2005:2679-2682.
360. Johannesen JK, Bi J, Jiang R, Kenney JG, Chen CA. Machine learning identification of EEG features predicting working memory performance in schizophrenia and healthy adults. *Neuropsychiatr Electrophysiol*. 2016;2:3. doi:10.1186/s40810-016-0017-0
361. Jin K, Xu D, Shen Z, et al. Distinguishing hypochondriasis and schizophrenia using regional homogeneity: a resting-state fMRI study and support vector machine analysis. *Acta Neuropsychiatr*. 2021;33(4):182-190. doi:10.1017/neu.2021.9
362. Siuly S, Khare SK, Bajaj V, Wang H, Zhang Y. A computerized method for automatic detection of schizophrenia using EEG signals. *IEEE Trans Neural Syst Rehabil Eng*. 2020;28(11):2390-2400. doi:10.1109/TNSRE.2020.3022715
363. Jang KI, Kim S, Kim SY, Lee C, Chae JH. Machine learning-based electroencephalographic phenotypes of schizophrenia and major depressive disorder. *Front Psychiatry*. 2021;12:745458. doi:10.3389/fpsy.2021.745458
364. Zheng J, Wei X, Wang J, Lin H, Pan H, Shi Y. Diagnosis of schizophrenia based on deep learning using fMRI. *Comput Math Methods Med*. 2021;2021:8437260. doi:10.1155/2021/8437260
365. Geenjaar E, Lewis N, Fu Z, Venkatdas R, Plis S, Calhoun V. Fusing multimodal neuroimaging data with a variational autoencoder. *Annu Int Conf IEEE Eng Med Biol Soc*. 2021;2021:3630-3633. doi:10.1109/EMBC46164.2021.9630806
366. Najafzadeh H, Esmaeili M, Farhang S, Sarbaz Y, Rasta SH. Automatic classification of schizophrenia patients using resting-state EEG signals. *Phys Eng Sci Med*. 2021;44(3):855-870. doi:10.1007/s13246-021-01038-7
367. Shoeibi A, Sadeghi D, Moridian P, et al. Automatic diagnosis of schizophrenia in EEG signals using CNN-LSTM models. *Front Neuroinform*. 2021;15:777977. doi:10.3389/fninf.2021.777977
368. Khare SK, Bajaj V. A self-learned decomposition and classification model for schizophrenia diagnosis. *Comput Methods Programs Biomed*. 2021;211:106450. doi:10.1016/j.cmpb.2021.106450
369. Lee LH, Chen CH, Chang WC, et al. Evaluating the performance of machine learning models for automatic diagnosis of patients with schizophrenia based on a single site dataset of 440 participants. *Eur Psychiatry*. 2021;65(1):e1. doi:10.1192/j.eurpsy.2021.2248
370. Wu J, Lyu G, Wang K, Tang X. A hybrid learning pipeline for automated diagnosis of first-episode schizophrenia utilizing T1-weighted images. *Annu Int Conf IEEE Eng Med Biol Soc*. 2021;2021:2761-2764. doi:10.1109/EMBC46164.2021.9630313
371. Hashimoto Y, Ogata Y, Honda M, Yamashita Y. Deep feature extraction for resting-state functional MRI by self-supervised learning and application to schizophrenia diagnosis. *Front Neurosci*. 2021;15:696853. doi:10.3389/fnins.2021.696853
372. Sharma M, Acharya UR. Automated detection of schizophrenia using optimal wavelet-based l1 norm features extracted from single-channel EEG. *Cogn Neurodyn*. 2021;15(4):661-674. doi:10.1007/s11571-020-09655-w
373. Al-Hiyali MI, Yahya N, Faye I, Hussein AF. Identification of autism subtypes based on wavelet coherence of BOLD fMRI signals using convolutional neural network. *Sensors (Basel)*. 2021;21(16):5256. doi:10.3390/s21165256
374. Elad D, Cetin-Karayumak S, Zhang F, et al. Improving the predictive potential of diffusion MRI in schizophrenia using normative models-towards subject-level classification. *Hum Brain Mapp*. 2021;42(14):4658-4670. doi:10.1002/hbm.25574
375. Wu Y, Ren P, Chen R, et al. Detection of functional and structural brain alterations in female schizophrenia using elastic net logistic regression. *Brain Imaging Behav*. 2022;16(1):281-290. doi:10.1007/s11682-021-00501-z
376. Cruz-Martinez C, Reyes-Garcia CA, Vanello N. A novel event-related fMRI supervoxels-based representation and its application to schizophrenia diagnosis. *Comput Methods Programs Biomed*. 2022;213:106509. doi:10.1016/j.cmpb.2021.106509
377. Algumaei AH, Algunaied RF, Rushdi MA, Yassine IA. Feature and decision-level fusion for schizophrenia detection based on resting-state fMRI data. *PLoS One*. 2022;17(5):e0265300. doi:10.1371/journal.pone.0265300

378. Tian Q, Yang NB, Fan Y, et al. Detection of schizophrenia cases from healthy controls with combination of neurocognitive and electrophysiological features. *Front Psychiatry*. 2022;13:810362. doi:10.3389/fpsy.2022.810362
379. Prabhakar SK, Rajaguru H, Kim C, Won DO. A fusion-based technique with hybrid swarm algorithm and deep learning for biosignal classification. *Front Hum Neurosci*. 2022;16:895761. doi:10.3389/fnhum.2022.895761
380. Khare SK, Bajaj V. A hybrid decision support system for automatic detection of schizophrenia using EEG signals. *Comput Biol Med*. 2022;141:105028. doi:10.1016/j.compbiomed.2021.105028
381. Zhou Z, Wang K, Tang J, et al. Cortical thickness distinguishes between major depression and schizophrenia in adolescents. *BMC Psychiatry*. 2021;21(1):361. doi:10.1186/s12888-021-03373-1
382. Li H, Cui L, Cao L, et al. Identification of bipolar disorder using a combination of multimodality magnetic resonance imaging and machine learning techniques. *BMC Psychiatry*. 2020;20(1):488. doi:10.1186/s12888-020-02886-5
383. Linke JO, Adleman NE, Sarlls J, et al. White matter microstructure in pediatric bipolar disorder and disruptive mood dysregulation disorder. *J Am Acad Child Adolesc Psychiatry*. 2020;59(10):1135-1145. doi:10.1016/j.jaac.2019.05.035
384. Squarcina L, Dagnew TM, Rivolta MW, Bellani M, Sassi R, Brambilla P. Automated cortical thickness and skewness feature selection in bipolar disorder using a semi-supervised learning method. *J Affect Disord*. 2019;256:416-423. doi:10.1016/j.jad.2019.06.019
385. Matsuo K, Harada K, Fujita Y, et al. Distinctive neuroanatomical substrates for depression in bipolar disorder versus major depressive disorder. *Cereb Cortex*. 2019;29(1):202-214. doi:10.1093/cercor/bhx319
386. Frangou S, Dima D, Jogie J. Towards person-centered neuroimaging markers for resilience and vulnerability in Bipolar Disorder. *Neuroimage*. 2017;145(Pt B):230-237. doi:10.1016/j.neuroimage.2016.08.066
387. Doan NT, Kaufmann T, Bettella F, et al. Distinct multivariate brain morphological patterns and their added predictive value with cognitive and polygenic risk scores in mental disorders. *Neuroimage Clin*. 2017;15:719-731. doi:10.1016/j.nicl.2017.06.014
388. Reavis EA, Lee J, Wynn JK, et al. Assessing neural tuning for object perception in schizophrenia and bipolar disorder with multivariate pattern analysis of fMRI data. *Neuroimage Clin*. 2017;16:491-497. doi:10.1016/j.nicl.2017.08.023
389. Mwangi B, Wu MJ, Bauer IE, et al. Predictive classification of pediatric bipolar disorder using atlas-based diffusion weighted imaging and support vector machines. *Psychiatry Res*. 2015;234(2):265-271. doi:10.1016/j.psychres.2015.10.002
390. Mwangi B, Spiker D, Zunta-Soares GB, Soares JC. Prediction of pediatric bipolar disorder using neuroanatomical signatures of the amygdala. *Bipolar Disord*. 2014;16(7):713-721. doi:10.1111/bdi.12222
391. Costafreda SG, Fu CH, Picchioni M, et al. Pattern of neural responses to verbal fluency shows diagnostic specificity for schizophrenia and bipolar disorder. *BMC Psychiatry*. 2011;11:18. doi:10.1186/1471-244X-11-18
392. Rashid B, Arbabshirani MR, Damaraju E, et al. Classification of schizophrenia and bipolar patients using static and dynamic resting-state fMRI brain connectivity. *Neuroimage*. 2016;134:645-657. doi:10.1016/j.neuroimage.2016.04.051
393. Kaufmann T, Alnæs D, Brandt CL, et al. Task modulations and clinical manifestations in the brain functional connectome in 1615 fMRI datasets. *Neuroimage*. 2017;147:243-252. doi:10.1016/j.neuroimage.2016.11.073
394. Mourão-Miranda J, Almeida JR, Hassel S, et al. Pattern recognition analyses of brain activation elicited by happy and neutral faces in unipolar and bipolar depression. *Bipolar Disord*. 2012;14(4):451-460. doi:10.1111/j.1399-5618.2012.01019.x
395. Wu MJ, Mwangi B, Bauer IE, et al. Identification and individualized prediction of clinical phenotypes in bipolar disorders using neurocognitive data, neuroimaging scans and machine learning. *Neuroimage*. 2017;145(Pt B):254-264. doi:10.1016/j.neuroimage.2016.02.016
396. Bürger C, Redlich R, Grotegerd D, et al. Differential abnormal pattern of anterior cingulate gyrus activation in unipolar and bipolar depression: an fMRI and pattern classification approach. *Neuropsychopharmacology*. 2017;42(7):1399-1408. doi:10.1038/npp.2017.36
397. Anticevic A, Cole MW, Repovs G, et al. Characterizing thalamo-cortical disturbances in schizophrenia and bipolar illness. *Cereb Cortex*. 2014;24(12):3116-3130. doi:10.1093/cercor/bht165
398. Besga A, Termenon M, Graña M, Echeveste J, Pérez JM, Gonzalez-Pinto A. Discovering Alzheimer's disease and bipolar disorder white matter effects building computer aided diagnostic systems on brain diffusion tensor imaging features. *Neurosci Lett*. 2012;520(1):71-76. doi:10.1016/j.neulet.2012.05.033

399. Chen Y, Storrs J, Tan L, Mazlack LJ, Lee JH, Lu LJ. Detecting brain structural changes as biomarker from magnetic resonance images using a local feature based SVM approach. *J Neurosci Methods*. 2014;221:22-31. doi:10.1016/j.jneumeth.2013.09.001
400. Xi C, Lai J, Du Y, et al. Abnormal functional connectivity within the reward network: a potential neuroimaging endophenotype of bipolar disorder. *J Affect Disord*. 2021;280(Pt B):49-56. doi:10.1016/j.jad.2020.11.072
401. Teng S, Lu CF, Wang PS, et al. Classification of bipolar disorder using basal-ganglia-related functional connectivity in the resting state. *Annu Int Conf IEEE Eng Med Biol Soc*. 2013;2013:1057-1060.
402. Nazhvani AD, Boostani R, Afrasiabi S, Sadatnezhad K. Classification of ADHD and BMD patients using visual evoked potential. *Clin Neurol Neurosurg*. 2013;115(11):2329-2335. doi:10.1016/j.clineuro.2013.08.009
403. Chen YL, Tu PC, Huang TH, et al. Using minimal-redundant and maximal-relevant whole-brain functional connectivity to classify bipolar disorder. *Front Neurosci*. 2020;14:563368. doi:10.3389/fnins.2020.563368
404. Mwangi B, Wu MJ, Cao B, et al. Individualized prediction and clinical staging of bipolar disorders using neuroanatomical biomarkers. *Biol Psychiatry Cogn Neurosci Neuroimaging*. 2016;1(2):186-194. doi:10.1016/j.bpsc.2016.01.001
405. Qiu Y, Yang M, Li S, et al. Altered fractional amplitude of low-frequency fluctuation in major depressive disorder and bipolar disorder. *Front Psychiatry*. 2021;12:739210. doi:10.3389/fpsy.2021.739210
406. Sánchez-Morla EM, Fuentes JL, Miguel-Jiménez JM, et al. Automatic diagnosis of bipolar disorder using optical coherence tomography data and artificial intelligence. *J Pers Med*. 2021;11(8):803. doi:10.3390/jpm11080803
407. Yamashita A, Sakai Y, Yamada T, et al. Generalizable brain network markers of major depressive disorder across multiple imaging sites. *PLoS Biol*. 2020;18(12):e3000966. doi:10.1371/journal.pbio.3000966
408. Maglanoc LA, Kaufmann T, Jonassen R, et al. Multimodal fusion of structural and functional brain imaging in depression using linked independent component analysis. *Hum Brain Mapp*. 2020;41(1):241-255. doi:10.1002/hbm.24802
409. Shim M, Jin MJ, Im CH, Lee SH. Machine-learning-based classification between post-traumatic stress disorder and major depressive disorder using P300 features. *Neuroimage Clin*. 2019;24:102001. doi:10.1016/j.nicl.2019.102001
410. Chun JY, Sendi MSE, Sui J, Zhi D, Calhoun VD. Visualizing functional network connectivity difference between healthy control and major depressive disorder using an explainable machine-learning method. *Annu Int Conf IEEE Eng Med Biol Soc*. 2020;2020:1424-1427. doi:10.1109/EMBC44109.2020.9175685
411. Uyulan C, Ergüzel TT, Unubol H, et al. Major depressive disorder classification based on different convolutional neural network models: deep learning approach. *Clin EEG Neurosci*. 2021;52(1):38-51. doi:10.1177/1550059420916634
412. Shi Y, Zhang L, Wang Z, et al. Multivariate machine learning analyses in identification of major depressive disorder using resting-state functional connectivity: a multicenter study. *ACS Chem Neurosci*. 2021;12(15):2878-2886. doi:10.1021/acchemneuro.1c00256
413. Mahato S, Goyal N, Ram D, Paul S. Detection of depression and scaling of severity using six channel EEG data. *J Med Syst*. 2020;44(7):118. doi:10.1007/s10916-020-01573-y
414. Guo H, Cao X, Liu Z, Li H, Chen J, Zhang K. Machine learning classifier using abnormal brain network topological metrics in major depressive disorder. *Neuroreport*. 2012;23(17):1006-1011. doi:10.1097/WNR.0b013e32835a650c
415. Guo H, Li Y, Mensah GK, et al. Resting-state functional network scale effects and statistical significance-based feature selection in machine learning classification. *Comput Math Methods Med*. 2019;2019:9108108. doi:10.1155/2019/9108108
416. Patel MJ, Andreescu C, Price JC, Edelman KL, Reynolds CF III, Aizenstein HJ. Machine learning approaches for integrating clinical and imaging features in late-life depression classification and response prediction. *Int J Geriatr Psychiatry*. 2015;30(10):1056-1067. doi:10.1002/gps.4262
417. Yang J, Zhang M, Ahn H, et al. Development and evaluation of a multimodal marker of major depressive disorder. *Hum Brain Mapp*. 2018;39(11):4420-4439. doi:10.1002/hbm.24282
418. Ahmadlou M, Adeli H, Adeli A. Fractality analysis of frontal brain in major depressive disorder. *Int J Psychophysiol*. 2012;85(2):206-211. doi:10.1016/j.ijpsycho.2012.05.001
419. Sacchet MD, Livermore EE, Iglesias JE, Glover GH, Gotlib IH. Subcortical volumes differentiate major depressive disorder, bipolar disorder, and remitted major depressive disorder. *J Psychiatr Res*. 2015;68:91-98. doi:10.1016/j.jpsychires.2015.06.002

420. Ramasubbu R, Brown EC, Marcil LD, Talai AS, Forkert ND. Automatic classification of major depression disorder using arterial spin labeling MRI perfusion measurements. *Psychiatry Clin Neurosci*. 2019;73(8):486-493. doi:10.1111/pcn.12862
421. Li H, Song S, Wang D, et al. Individualized diagnosis of major depressive disorder via multivariate pattern analysis of thalamic sMRI features. *BMC Psychiatry*. 2021;21(1):415. doi:10.1186/s12888-021-03414-9
422. Zhong X, Shi H, Ming Q, et al. Whole-brain resting-state functional connectivity identified major depressive disorder: a multivariate pattern analysis in two independent samples. *J Affect Disord*. 2017;218:346-352. doi:10.1016/j.jad.2017.04.040
423. Liu W, Zhang C, Wang X, et al. Functional connectivity of major depression disorder using ongoing EEG during music perception. *Clin Neurophysiol*. 2020;131(10):2413-2422. doi:10.1016/j.clinph.2020.06.031
424. Liao SC, Wu CT, Huang HC, Cheng WT, Liu YH. Major depression detection from EEG signals using kernel Eigen-filter-bank common spatial patterns. *Sensors (Basel)*. 2017;17(6):1385. doi:10.3390/s17061385
425. Rosa MJ, Portugal L, Hahn T, et al. Sparse network-based models for patient classification using fMRI. *Neuroimage*. 2015;105:493-506. doi:10.1016/j.neuroimage.2014.11.021
426. Schnyer DM, Clasen PC, Gonzalez C, Beevers CG. Evaluating the diagnostic utility of applying a machine learning algorithm to diffusion tensor MRI measures in individuals with major depressive disorder. *Psychiatry Res Neuroimaging*. 2017;264:1-9. doi:10.1016/j.psychres.2017.03.003
427. Johnston BA, Steele JD, Tolomeo S, Christmas D, Matthews K. Structural MRI-based predictions in patients with treatment-refractory depression (TRD). *PLoS One*. 2015;10(7):e0132958. doi:10.1371/journal.pone.0132958
428. Liu F, Guo W, Yu D, et al. Classification of different therapeutic responses of major depressive disorder with multivariate pattern analysis method based on structural MR scans. *PLoS One*. 2012;7(7):e40968. doi:10.1371/journal.pone.0040968
429. Wei M, Qin J, Yan R, Li H, Yao Z, Lu Q. Identifying major depressive disorder using Hurst exponent of resting-state brain networks. *Psychiatry Res*. 2013;214(3):306-312. doi:10.1016/j.psychres.2013.09.008
430. Chu SH, Lenglet C, Schreiner MW, Klimes-Dougan B, Cullen K, Parhi KK. Anatomical biomarkers for adolescent major depressive disorder from diffusion weighted imaging using SVM classifier. *Annu Int Conf IEEE Eng Med Biol Soc*. 2018;2018:2740-2743. doi:10.1109/EMBC.2018.8512852
431. Guo H, Qin M, Chen J, Xu Y, Xiang J. Machine-learning classifier for patients with major depressive disorder: multifeature approach based on a high-order minimum spanning tree functional brain network. *Comput Math Methods Med*. 2017;2017:4820935. doi:10.1155/2017/4820935
432. Zeng LL, Shen H, Liu L, Hu D. Unsupervised classification of major depression using functional connectivity MRI. *Hum Brain Mapp*. 2014;35(4):1630-1641. doi:10.1002/hbm.22278
433. Fang P, Zeng LL, Shen H, et al. Increased cortical-limbic anatomical network connectivity in major depression revealed by diffusion tensor imaging. *PLoS One*. 2012;7(9):e45972. doi:10.1371/journal.pone.0045972
434. Tan W, Liu Z, Xi C, et al. Decreased integration of the frontoparietal network during a working memory task in major depressive disorder. *Aust N Z J Psychiatry*. 2021;55(6):577-587. doi:10.1177/0004867420978284
435. Cao L, Guo S, Xue Z, et al. Aberrant functional connectivity for diagnosis of major depressive disorder: a discriminant analysis. *Psychiatry Clin Neurosci*. 2014;68(2):110-119. doi:10.1111/pcn.12106
436. Zeng LL, Shen H, Liu L, et al. Identifying major depression using whole-brain functional connectivity: a multivariate pattern analysis. *Brain*. 2012;135(Pt 5):1498-1507. doi:10.1093/brain/aws059
437. Ramasubbu R, Brown MR, Cortese F, et al. Accuracy of automated classification of major depressive disorder as a function of symptom severity. *Neuroimage Clin*. 2016;12:320-331. doi:10.1016/j.nicl.2016.07.012
438. Qiu L, Huang X, Zhang J, et al. Characterization of major depressive disorder using a multiparametric classification approach based on high resolution structural images. *J Psychiatry Neurosci*. 2014;39(2):78-86.
439. Mwangi B, Ebmeier KP, Matthews K, Steele JD. Multi-centre diagnostic classification of individual structural neuroimaging scans from patients with major depressive disorder. *Brain*. 2012;135(Pt 5):1508-1521. doi:10.1093/brain/aws084
440. Zhao J, Huang J, Zhi D, et al. Functional network connectivity (FNC)-based generative adversarial network (GAN) and its applications in classification of mental disorders. *J Neurosci Methods*. 2020;341:108756. doi:10.1016/j.jneumeth.2020.108756
441. Bi K, Hua L, Wei M, Qin J, Lu Q, Yao Z. Dynamic functional-structural coupling within acute functional state change phases: evidence from a depression recognition study. *J Affect Disord*. 2016;191:145-155. doi:10.1016/j.jad.2015.11.041

442. Zhu X, Yuan F, Zhou G, et al. Cross-network interaction for diagnosis of major depressive disorder based on resting state functional connectivity. *Brain Imaging Behav.* 2021;15(3):1279-1289. doi:10.1007/s11682-020-00326-2
443. Sundermann B, Feder S, Wersching H, et al. Diagnostic classification of unipolar depression based on resting-state functional connectivity MRI: effects of generalization to a diverse sample. *J Neural Transm (Vienna).* 2017; 124(5):589-605. doi:10.1007/s00702-016-1673-8
444. Qin J, Wei M, Liu H, et al. Abnormal hubs of white matter networks in the frontal-parieto circuit contribute to depression discrimination via pattern classification. *Magn Reson Imaging.* 2014;32(10):1314-1320. doi:10.1016/j.mri.2014.08.037
445. Guo M, Wang T, Zhang Z, et al. Diagnosis of major depressive disorder using whole-brain effective connectivity networks derived from resting-state functional MRI. *J Neural Eng.* 2020;17(5):056038. doi:10.1088/1741-2552/abbc28
446. Khan D, Yahya N, Kamel N, Faye I. Automated diagnosis of major depressive disorder using brain effective connectivity and 3D convolutional neural network. *IEEE Access.* 2021;(9):8835-8846. doi:10.1109/ACCESS.2021.3049427
447. Zhang B, Yan G, Yang Z, Su Y, Wang J, Lei T. Brain functional networks based on resting-state EEG data for major depressive disorder analysis and classification. *IEEE Trans Neural Syst Rehabil Eng.* 2021;29:215-229. doi:10.1109/TNSRE.2020.3043426
448. Zhu Y, Jayagopal JK, Mehta RK, et al. Classifying major depressive disorder using fNIRS during motor rehabilitation. *IEEE Trans Neural Syst Rehabil Eng.* 2020;28(4):961-969. doi:10.1109/TNSRE.2020.2972270
449. Geng X, Xu J, Liu B, Shi Y. Multivariate classification of major depressive disorder using the effective connectivity and functional connectivity. *Front Neurosci.* 2018;12:38. doi:10.3389/fnins.2018.00038
450. Sacchet MD, Prasad G, Foland-Ross LC, Thompson PM, Gotlib IH. Elucidating brain connectivity networks in major depressive disorder using classification-based scoring. *Proc IEEE Int Symp Biomed Imaging.* 2014;2014: 246-249. doi:10.1109/ISBI.2014.6867855
451. Yan B, Xu X, Liu M, et al. Quantitative identification of major depression based on resting-state dynamic functional connectivity: a machine learning approach. *Front Neurosci.* 2020;14:191. doi:10.3389/fnins.2020.00191
452. Nakano T, Takamura M, Ichikawa N, et al. Enhancing multi-center generalization of machine learning-based depression diagnosis from resting-state fMRI. *Front Psychiatry.* 2020;11:400. doi:10.3389/fpsy.2020.00400
453. Sacchet MD, Prasad G, Foland-Ross LC, Thompson PM, Gotlib IH. Support vector machine classification of major depressive disorder using diffusion-weighted neuroimaging and graph theory. *Front Psychiatry.* 2015;6:21. doi:10.3389/fpsy.2015.00021
454. Shi Y, Zhang L, He C, et al. Sleep disturbance-related neuroimaging features as potential biomarkers for the diagnosis of major depressive disorder: a multicenter study based on machine learning. *J Affect Disord.* 2021;295: 148-155. doi:10.1016/j.jad.2021.08.027
455. Duan L, Duan H, Qiao Y, et al. Machine learning approaches for MDD detection and emotion decoding using EEG signals. *Front Hum Neurosci.* 2020;14:284. doi:10.3389/fnhum.2020.00284
456. Saeedi A, Saeedi M, Maghsoudi A, Shalbfaf A. Major depressive disorder diagnosis based on effective connectivity in EEG signals: a convolutional neural network and long short-term memory approach. *Cogn Neurodyn.* 2021;15(2):239-252. doi:10.1007/s11571-020-09619-0
457. Bi K, Chattun MR, Liu X, et al. Abnormal early dynamic individual patterns of functional networks in low gamma band for depression recognition. *J Affect Disord.* 2018;238:366-374. doi:10.1016/j.jad.2018.05.078
458. Qin J, Wei M, Liu H, et al. Altered anatomical patterns of depression in relation to antidepressant treatment: evidence from a pattern recognition analysis on the topological organization of brain networks. *J Affect Disord.* 2015;180:129-137. doi:10.1016/j.jad.2015.03.059
459. Knott V, Mahoney C, Kennedy S, Evans K. EEG power, frequency, asymmetry and coherence in male depression. *Psychiatry Res.* 2001;106(2):123-140. doi:10.1016/S0925-4927(00)00080-9
460. Marquand AF, Mourão-Miranda J, Brammer MJ, Cleare AJ, Fu CH. Neuroanatomy of verbal working memory as a diagnostic biomarker for depression. *Neuroreport.* 2008;19(15):1507-1511. doi:10.1097/WNR.0b013e328310425e
461. Lu Q, Bi K, Liu C, Luo G, Tang H, Yao Z. Predicting depression based on dynamic regional connectivity: a windowed Granger causality analysis of MEG recordings. *Brain Res.* 2013;1535:52-60. doi:10.1016/j.brainres.2013.08.033
462. Craddock RC, Holtzheimer PE III, Hu XP, Mayberg HS. Disease state prediction from resting state functional connectivity. *Magn Reson Med.* 2009;62(6):1619-1628. doi:10.1002/mrm.22159

463. Kang M, Kwon H, Park JH, Kang S, Lee Y. Deep-asymmetry: asymmetry matrix image for deep learning method in pre-screening depression. *Sensors (Basel)*. 2020;20(22):6526. doi:10.3390/s20226526
464. Lois G, Wessa M. Differential association of default mode network connectivity and rumination in healthy individuals and remitted MDD patients. *Soc Cogn Affect Neurosci*. 2016;11(11):1792-1801. doi:10.1093/scan/nsw085
465. Hasanzadeh F, Mohebbi M, Rostami R. Graph theory analysis of directed functional brain networks in major depressive disorder based on EEG signal. *J Neural Eng*. 2020;17(2):026010. doi:10.1088/1741-2552/ab7613
466. Mumtaz W, Ali SSA, Yasin MAM, Malik AS. A machine learning framework involving EEG-based functional connectivity to diagnose major depressive disorder (MDD). *Med Biol Eng Comput*. 2018;56(2):233-246. doi:10.1007/s11517-017-1685-z
467. Sen B, Cullen KR, Parhi KK. Classification of adolescent major depressive disorder via static and dynamic connectivity. *IEEE J Biomed Health Inform*. 2021;25(7):2604-2614. doi:10.1109/JBHI.2020.3043427
468. Movahed RA, Jahromi GP, Shahyad S, Meftahi GH. A major depressive disorder classification framework based on EEG signals using statistical, spectral, wavelet, functional connectivity, and nonlinear analysis. *J Neurosci Methods*. 2021;358:109209. doi:10.1016/j.jneumeth.2021.109209
469. Li Y, Dai X, Wu H, Wang L. Establishment of effective biomarkers for depression diagnosis with fusion of multiple resting-state connectivity measures. *Front Neurosci*. 2021;15:729958. doi:10.3389/fnins.2021.729958
470. Wu CT, Huang HC, Huang S, et al. Resting-state EEG signal for major depressive disorder detection: a systematic validation on a large and diverse dataset. *Biosensors (Basel)*. 2021;11(12):499. doi:10.3390/bios11120499
471. Gao Y, Wang X, Xiong Z, et al. Abnormal fractional amplitude of low-frequency fluctuation as a potential imaging biomarker for first-episode major depressive disorder: a resting-state fMRI study and support vector machine analysis. *Front Neurol*. 2021;12:751400. doi:10.3389/fneur.2021.751400
472. Lin H, Jian C, Cao Y, et al. MDD-TSVM: a novel semisupervised-based method for major depressive disorder detection using electroencephalogram signals. *Comput Biol Med*. 2021;140:105039. doi:10.1016/j.combiomed.2021.105039
473. Liu B, Chang H, Peng K, Wang X. An end-to-end depression recognition method based on EEGNet. *Front Psychiatry*. 2022;13:864393. doi:10.3389/fpsy.2022.864393
474. Frick A, Gingnell M, Marquand AF, et al. Classifying social anxiety disorder using multivoxel pattern analyses of brain function and structure. *Behav Brain Res*. 2014;259:330-335. doi:10.1016/j.bbr.2013.11.003
475. Zhang W, Yang X, Lui S, et al. Diagnostic prediction for social anxiety disorder via multivariate pattern analysis of the regional homogeneity. *Biomed Res Int*. 2015;2015:763965. doi:10.1155/2015/763965
476. Liu F, Guo W, Fouche JP, et al. Multivariate classification of social anxiety disorder using whole brain functional connectivity. *Brain Struct Funct*. 2015;220(1):101-115. doi:10.1007/s00429-013-0641-4
477. Xing M, Fitzgerald JM, Klumpp H. Classification of social anxiety disorder with support vector machine analysis using neural correlates of social signals of threat. *Front Psychiatry*. 2020;11:144. doi:10.3389/fpsy.2020.00144
478. Gavrilescu M, Vizireanu N. Predicting depression, anxiety, and stress levels from videos using the facial action coding system. *Sensors (Basel)*. 2019;19(17):3693. doi:10.3390/s19173693
479. Xie Y, Yang B, Lu X, et al. Anxiety and depression diagnosis method based on brain networks and convolutional neural networks. *Annu Int Conf IEEE Eng Med Biol Soc*. 2020;2020:1503-1506. doi:10.1109/EMBC44109.2020.9176471
480. Qiao J, Li A, Cao C, Wang Z, Sun J, Xu G. Aberrant functional network connectivity as a biomarker of generalized anxiety disorder. *Front Hum Neurosci*. 2017;11:626. doi:10.3389/fnhum.2017.00626
481. Xing X, Jin L, Li Q, et al. Modeling essential connections in obsessive-compulsive disorder patients using functional MRI. *Brain Behav*. 2020;10(2):e01499. doi:10.1002/brb3.1499
482. Yang X, Hu X, Tang W, et al. Multivariate classification of drug-naive obsessive-compulsive disorder patients and healthy controls by applying an SVM to resting-state functional MRI data. *BMC Psychiatry*. 2019;19(1):210. doi:10.1186/s12888-019-2184-6
483. Bruin WB, Taylor L, Thomas RM, et al; ENIGMA-OCD Working Group. Structural neuroimaging biomarkers for obsessive-compulsive disorder in the ENIGMA-OCD consortium: medication matters. *Transl Psychiatry*. 2020;10(1):342. doi:10.1038/s41398-020-01013-y
484. Takagi Y, Sakai Y, Lisi G, et al. A neural marker of obsessive-compulsive disorder from whole-brain functional connectivity. *Sci Rep*. 2017;7(1):7538. doi:10.1038/s41598-017-07792-7

485. Zhou C, Cheng Y, Ping L, et al. Support vector machine classification of obsessive-compulsive disorder based on whole-brain volumetry and diffusion tensor imaging. *Front Psychiatry*. 2018;9:524. doi:10.3389/fpsy.2018.00524
486. Hu X, Liu Q, Li B, et al. Multivariate pattern analysis of obsessive-compulsive disorder using structural neuroanatomy. *Eur Neuropsychopharmacol*. 2016;26(2):246-254. doi:10.1016/j.euroneuro.2015.12.014
487. Bu X, Hu X, Zhang L, et al. Investigating the predictive value of different resting-state functional MRI parameters in obsessive-compulsive disorder. *Transl Psychiatry*. 2019;9(1):17. doi:10.1038/s41398-018-0362-9
488. Sen B, Bernstein GA, Tingting X, et al. Classification of obsessive-compulsive disorder from resting-state fMRI. *Annu Int Conf IEEE Eng Med Biol Soc*. 2016;2016:3606-3609. doi:10.1109/EMBC.2016.7591508
489. Trambaiolli LR, Biazoli CE Jr, Balardin JB, Hoexter MQ, Sato JR. The relevance of feature selection methods to the classification of obsessive-compulsive disorder based on volumetric measures. *J Affect Disord*. 2017;222:49-56. doi:10.1016/j.jad.2017.06.061
490. Li F, Huang X, Tang W, et al. Multivariate pattern analysis of DTI reveals differential white matter in individuals with obsessive-compulsive disorder. *Hum Brain Mapp*. 2014;35(6):2643-2651. doi:10.1002/hbm.22357
491. Shen SK, Halici U, Çiçek M. A comparative analysis of functional connectivity data in resting and task-related conditions of the brain for disease signature of OCD. *Annu Int Conf IEEE Eng Med Biol Soc*. 2014;2014:978-981. doi:10.1109/EMBC.2014.6943756
492. Liu J, Bu X, Hu X, et al. Temporal variability of regional intrinsic neural activity in drug-naïve patients with obsessive-compulsive disorder. *Hum Brain Mapp*. 2021;42(12):3792-3803. doi:10.1002/hbm.25465
493. Liu W, Hua M, Qin J, et al. Disrupted pathways from frontal-parietal cortex to basal ganglia and cerebellum in patients with unmedicated obsessive compulsive disorder as observed by whole-brain resting-state effective connectivity analysis: a small sample pilot study. *Brain Imaging Behav*. 2021;15(3):1344-1354. doi:10.1007/s11682-020-00333-3
494. Chen Y, Ou Y, Lv D, et al. Decreased nucleus accumbens connectivity at rest in medication-free patients with obsessive-compulsive disorder. *Neural Plast*. 2021;2021:9966378. doi:10.1155/2021/9966378
495. Kalatzis I, Piliouras N, Glotsos D, et al. Identifying differences in the P600 component of ERP-signals between OCD patients and controls employing a PNN-based majority vote classification scheme. *Conf Proc IEEE Eng Med Biol Soc*. 2005;2005:3994-3997. doi:10.1109/IEMBS.2005.1615337
496. Aydin S, Arica N, Ergul E, Tan O. Classification of obsessive compulsive disorder by EEG complexity and hemispheric dependency measurements. *Int J Neural Syst*. 2015;25(3):1550010. doi:10.1142/S0129065715500100
497. Zilcha-Mano S, Zhu X, Suarez-Jimenez B, et al. Diagnostic and predictive neuroimaging biomarkers for posttraumatic stress disorder. *Biol Psychiatry Cogn Neurosci Neuroimaging*. 2020;5(7):688-696. doi:10.1016/j.bpsc.2020.03.010
498. Nicholson AA, Densmore M, McKinnon MC, et al. Machine learning multivariate pattern analysis predicts classification of posttraumatic stress disorder and its dissociative subtype: a multimodal neuroimaging approach. *Psychol Med*. 2019;49(12):2049-2059. doi:10.1017/S0033291718002866
499. Zhu H, Yuan M, Qiu C, et al. Multivariate classification of earthquake survivors with post-traumatic stress disorder based on large-scale brain networks. *Acta Psychiatr Scand*. 2020;141(3):285-298. doi:10.1111/acps.13150
500. Nicholson AA, Harricharan S, Densmore M, et al. Classifying heterogeneous presentations of PTSD via the default mode, central executive, and salience networks with machine learning. *Neuroimage Clin*. 2020;27:102262. doi:10.1016/j.nicl.2020.102262
501. Harricharan S, Nicholson AA, Thome J, et al. PTSD and its dissociative subtype through the lens of the insula: anterior and posterior insula resting-state functional connectivity and its predictive validity using machine learning. *Psychophysiology*. 2020;57(1):e13472. doi:10.1111/psyp.13472
502. Yang J, Lei D, Qin K, et al. Using deep learning to classify pediatric posttraumatic stress disorder at the individual level. *BMC Psychiatry*. 2021;21(1):535. doi:10.1186/s12888-021-03503-9
503. Chen Z, Feng P, Becker B, et al. Neural connectome prospectively encodes the risk of post-traumatic stress disorder (PTSD) symptom during the COVID-19 pandemic. *Neurobiol Stress*. 2021;15:100378. doi:10.1016/j.yjnstr.2021.100378
504. Eken A, Çolak B, Bal NB, et al. Hyperparameter-tuned prediction of somatic symptom disorder using functional near-infrared spectroscopy-based dynamic functional connectivity. *J Neural Eng*. 2019;17(1):016012. doi:10.1088/1741-2552/ab50b2

505. Lavagnino L, Amianto F, Mwangi B, et al. Identifying neuroanatomical signatures of anorexia nervosa: a multivariate machine learning approach. *Psychol Med*. 2015;45(13):2805-2812. doi:10.1017/S0033291715000768
506. Lavagnino L, Mwangi B, Cao B, Shott ME, Soares JC, Frank GKW. Cortical thickness patterns as state biomarker of anorexia nervosa. *Int J Eat Disord*. 2018;51(3):241-249. doi:10.1002/eat.22828
507. Geisler D, Borchardt V, Boehm I, et al. Altered global brain network topology as a trait marker in patients with anorexia nervosa. *Psychol Med*. 2020;50(1):107-115. doi:10.1017/S0033291718004002
508. Weygandt M, Schaefer A, Schienle A, Haynes JD. Diagnosing different binge-eating disorders based on reward-related brain activation patterns. *Hum Brain Mapp*. 2012;33(9):2135-2146. doi:10.1002/hbm.21345
509. Lee MH, Kim N, Yoo J, et al. Multitask fMRI and machine learning approach improve prediction of differential brain activity pattern in patients with insomnia disorder. *Sci Rep*. 2021;11(1):9402. doi:10.1038/s41598-021-88845-w
510. Jansen C, Penzel T, Hodel S, Breuer S, Spott M, Krefting D. Network physiology in insomnia patients: assessment of relevant changes in network topology with interpretable machine learning models. *Chaos*. 2019;29(12):123129. doi:10.1063/1.5128003
511. Zhang J, Liu Y, Luo R, et al. Classification of pure conduct disorder from healthy controls based on indices of brain networks during resting state. *Med Biol Eng Comput*. 2020;58(9):2071-2082. doi:10.1007/s11517-020-02215-8
512. Zhang J, Cao W, Wang M, Wang N, Yao S, Huang B. Multivoxel pattern analysis of structural MRI in children and adolescents with conduct disorder. *Brain Imaging Behav*. 2019;13(5):1273-1280. doi:10.1007/s11682-018-9953-6
513. Zhang J, Liu W, Zhang J, et al. Distinguishing adolescents with conduct disorder from typically developing youngsters based on pattern classification of brain structural MRI. *Front Hum Neurosci*. 2018;12:152. doi:10.3389/fnhum.2018.00152
514. Tang Y, Jiang W, Liao J, Wang W, Luo A. Identifying individuals with antisocial personality disorder using resting-state FMRI. *PLoS One*. 2013;8(4):e60652. doi:10.1371/journal.pone.0060652
515. Tang Y, Liu W, Chen J, Liao J, Hu D, Wang W. Altered spontaneous activity in antisocial personality disorder revealed by regional homogeneity. *Neuroreport*. 2013;24(11):590-595. doi:10.1097/WNR.0b013e3283627993
516. Sato JR, de Oliveira-Souza R, Thomaz CE, et al. Identification of psychopathic individuals using pattern classification of MRI images. *Soc Neurosci*. 2011;6(5-6):627-639. doi:10.1080/17470919.2011.562687
517. Wetherill RR, Rao H, Hager N, Wang J, Franklin TR, Fan Y. Classifying and characterizing nicotine use disorder with high accuracy using machine learning and resting-state fMRI. *Addict Biol*. 2019;24(4):811-821. doi:10.1111/adb.12644
518. Li Y, Cui Z, Liao Q, et al. Support vector machine-based multivariate pattern classification of methamphetamine dependence using arterial spin labeling. *Addict Biol*. 2019;24(6):1254-1262. doi:10.1111/adb.12705
519. Ding X, Li Y, Li D, Li L, Liu X. Using machine-learning approach to distinguish patients with methamphetamine dependence from healthy subjects in a virtual reality environment. *Brain Behav*. 2020;10(11):e01814. doi:10.1002/brb3.1814
520. Mete M, Sakoglu U, Spence JS, Devous MD Sr, Harris TS, Adinoff B. Successful classification of cocaine dependence using brain imaging: a generalizable machine learning approach. *BMC Bioinformatics*. 2016;17(suppl 13):357. doi:10.1186/s12859-016-1218-z
521. Adeli E, Zahr NM, Pfefferbaum A, Sullivan EV, Pohl KM. Novel machine learning identifies brain patterns distinguishing diagnostic membership of human immunodeficiency virus, alcoholism, and their comorbidity of individuals. *Biol Psychiatry Cogn Neurosci Neuroimaging*. 2019;4(6):589-599. doi:10.1016/j.bpsc.2019.02.003
522. Guggenmos M, Schmack K, Veer IM, et al. A multimodal neuroimaging classifier for alcohol dependence. *Sci Rep*. 2020;10(1):298. doi:10.1038/s41598-019-56923-9
523. Mehla VK, Singhal A, Singh P. A novel approach for automated alcoholism detection using Fourier decomposition method. *J Neurosci Methods*. 2020;346:108945. doi:10.1016/j.jneumeth.2020.108945
524. Zhu X, Du X, Kerich M, Lohoff FW, Momenan R. Random forest based classification of alcohol dependence patients and healthy controls using resting state MRI. *Neurosci Lett*. 2018;676:27-33. doi:10.1016/j.neulet.2018.04.007
525. Mumtaz W, Saad MNBM, Kamel N, Ali SSA, Malik AS. An EEG-based functional connectivity measure for automatic detection of alcohol use disorder. *Artif Intell Med*. 2018;84:79-89. doi:10.1016/j.artmed.2017.11.002

526. Wang SH, Lv YD, Sui Y, Liu S, Wang SJ, Zhang YD. Alcoholism detection by data augmentation and convolutional neural network with stochastic pooling. *J Med Syst*. 2017;42(1):2. doi:10.1007/s10916-017-0845-x
527. Kinreich S, McCutcheon VV, Aliev F, et al. Predicting alcohol use disorder remission: a longitudinal multimodal multi-featured machine learning approach. *Transl Psychiatry*. 2021;11(1):166. doi:10.1038/s41398-021-01281-2
528. Bae Y, Yoo BW, Lee JC, Kim HC. Automated network analysis to measure brain effective connectivity estimated from EEG data of patients with alcoholism. *Physiol Meas*. 2017;38(5):759-773. doi:10.1088/1361-6579/aa6b4c
529. Kumar S, Ghosh S, Tatarway S, Sinha RK. Support vector machine and fuzzy C-mean clustering-based comparative evaluation of changes in motor cortex electroencephalogram under chronic alcoholism. *Med Biol Eng Comput*. 2015;53(7):609-622. doi:10.1007/s11517-015-1264-0
530. Khan DM, Yahya N, Kamel N, Faye I. Effective connectivity in default mode network for alcoholism diagnosis. *IEEE Trans Neural Syst Rehabil Eng*. 2021;29:796-808. doi:10.1109/TNSRE.2021.3075737
531. Mumtaz W, Vuong PL, Xia L, Malik AS, Rashid RBA. An EEG-based machine learning method to screen alcohol use disorder. *Cogn Neurodyn*. 2017;11(2):161-171. doi:10.1007/s11571-016-9416-y
532. Hahn S, Mackey S, Cousijn J, et al. Predicting alcohol dependence from multi-site brain structural measures. *Hum Brain Mapp*. 2022;43(1):555-565. doi:10.1002/hbm.25248
533. Zhang H, Silva FHS, Ohata EF, Medeiros AG, Rebouças Filho PP. Bi-dimensional approach based on transfer learning for alcoholism pre-disposition classification via EEG signals. *Front Hum Neurosci*. 2020;14:365. doi:10.3389/fnhum.2020.00365
534. Wang SH, Xie S, Chen X, et al. Alcoholism identification based on an AlexNet transfer learning model. *Front Psychiatry*. 2019;10:205. doi:10.3389/fpsy.2019.00205
535. Prabhakar SK, Rajaguru H. Alcoholic EEG signal classification with correlation dimension based distance metrics approach and modified Adaboost classification. *Heliyon*. 2020;6(12):e05689. doi:10.1016/j.heliyon.2020.e05689
536. Dai X, Gao L, Zhang H, Wei X, Liu Z. A combination of support vector machine and voxel-based morphometry in adult male alcohol use disorder patients with cognitive deficits. *Brain Res*. 2021;1771:147644. doi:10.1016/j.brainres.2021.147644
537. Erguzel TT, Noyan CO, Eryilmaz G, et al. Binomial logistic regression and artificial neural network methods to classify opioid-dependent subjects and control group using quantitative EEG power measures. *Clin EEG Neurosci*. 2019;50(5):303-310. doi:10.1177/1550059418824450
538. Cremers H, van Zutphen L, Duken S, et al. Borderline personality disorder classification based on brain network measures during emotion regulation. *Eur Arch Psychiatry Clin Neurosci*. 2021;271(6):1169-1178. doi:10.1007/s00406-020-01201-3
539. Xu T, Cullen KR, Hourri A, Lim KO, Schulz SC, Parhi KK. Classification of borderline personality disorder based on spectral power of resting-state fMRI. *Annu Int Conf IEEE Eng Med Biol Soc*. 2014;2014:5036-5039.
540. Grecucci A, Lapomarda G, Messina I, Monachesi B, Sorella S, Siugzdaitė R. Structural features related to affective instability correctly classify patients with borderline personality disorder: a supervised machine learning approach. *Front Psychiatry*. 2022;13:804440. doi:10.3389/fpsy.2022.804440
541. Menon SS, Krishnamurthy K. Multimodal ensemble deep learning to predict disruptive behavior disorders in children. *Front Neuroinform*. 2021;15:742807. doi:10.3389/fninf.2021.742807
542. Page MJ, Moher D, Bossuyt PM, et al. PRISMA 2020 explanation and elaboration: updated guidance and exemplars for reporting systematic reviews. *BMJ*. 2021;372(160):n160. doi:10.1136/bmj.n160
543. Stroup DF, Berlin JA, Morton SC, et al. Meta-analysis of observational studies in epidemiology: a proposal for reporting. Meta-analysis of Observational Studies in Epidemiology (MOOSE) group. *JAMA*. 2000;283(15):2008-2012. doi:10.1001/jama.283.15.2008
544. Moons KG, de Groot JA, Bouwmeester W, et al. Critical appraisal and data extraction for systematic reviews of prediction modelling studies: the CHARMS checklist. *PLoS Med*. 2014;11(10):e1001744. doi:10.1371/journal.pmed.1001744
545. Venema E, Wessler BS, Paulus JK, et al. Large-scale validation of the prediction model risk of bias assessment tool (PROBAST) using a short form: high risk of bias models show poorer discrimination. *J Clin Epidemiol*. 2021;138:32-39. doi:10.1016/j.jclinepi.2021.06.017
546. Di Tanna GL, Wirtz H, Burrows KL, Globe G. Evaluating risk prediction models for adults with heart failure: a systematic literature review. *PLoS One*. 2020;15(1):e0224135. doi:10.1371/journal.pone.0224135
547. Du M, Haag D, Song Y, Lynch J, Mittinty M. Examining bias and reporting in oral health prediction modeling studies. *J Dent Res*. 2020;99(4):374-387. doi:10.1177/0022034520903725

548. Varoquaux G. Cross-validation failure: small sample sizes lead to large error bars. *NeuroImage*. 2018;180(pt A):68-77. doi:10.1016/j.neuroimage.2017.06.061
549. Janssen RJ, Mourão-Miranda J, Schnack HG. Making individual prognoses in psychiatry using neuroimaging and machine learning. *Biol Psychiatry Cogn Neurosci Neuroimaging*. 2018;3(9):798-808. doi:10.1016/j.bpsc.2018.04.004
550. Jollans L, Boyle R, Artiges E, et al. Quantifying performance of machine learning methods for neuroimaging data. *Neuroimage*. 2019;199:351-365. doi:10.1016/j.neuroimage.2019.05.082
551. Poldrack RA, Huckins G, Varoquaux G. Establishment of best practices for evidence for prediction: a review. *JAMA Psychiatry*. 2020;77(5):534-540. doi:10.1001/jamapsychiatry.2019.3671
552. Flint C, Cearns M, Opel N, et al. Systematic misestimation of machine learning performance in neuroimaging studies of depression. *Neuropsychopharmacology*. 2021;46(8):1510-1517. doi:10.1038/s41386-021-01020-7
553. Samala RK, Chan H-P, Hadjiiski L, Koneru S. Hazards of data leakage in machine learning: a study on classification of breast cancer using deep neural networks. In: Hahn HK, Mazurowski MA, eds. *Medical Imaging 2020: Computer-Aided Diagnosis*. Proceedings of the SPIE. Volume 11314. SPIE; 2020:1131416.
554. Chapelle O, Vapnik VN, Bousquet O, Mukherjee SJML. Choosing multiple parameters for support vector machines. *Machine Language*. 2002;46(1):131-159.
555. Baydin AG, Pearlmutter BA, Siskind JM. Tricks from deep learning. *arXiv*. Preprint posted online November 10, 2016.
556. Zhang C, Bengio S, Hardt M, Recht B, Vinyals O. Understanding deep learning (still) requires rethinking generalization. *Commun ACM*. 2021;64(3):107-115. doi:10.1145/3446776
557. Breck E, Cai S, Nielsen E, Salib M, Sculley D. The ML test score: a rubric for ML production readiness and technical debt reduction. *Proceedings of IEEE Big Data*. 2017:1123-1132.
558. Sendak MP, Gao M, Brajer N, Balu S. Presenting machine learning model information to clinical end users with model facts labels. *NPJ Digit Med*. 2020;3(1):41. doi:10.1038/s41746-020-0253-3
559. Heus P, Damen JAAG, Pajouheshnia R, et al. Poor reporting of multivariable prediction model studies: towards a targeted implementation strategy of the TRIPOD statement. *BMC Med*. 2018;16(1):120. doi:10.1186/s12916-018-1099-2
560. Groot OQ, Ogink PT, Lans A, et al. Machine learning prediction models in orthopedic surgery: a systematic review in transparent reporting. *J Orthop Res*. 2022;40(2):475-483. doi:10.1002/jor.25036
561. Dhiman P, Ma J, Navarro CA, et al. Reporting of prognostic clinical prediction models based on machine learning methods in oncology needs to be improved. *J Clin Epidemiol*. 2021;138:60-72. doi:10.1016/j.jclinepi.2021.06.024
562. Collins GS, Dhiman P, Andaur Navarro CL, et al. Protocol for development of a reporting guideline (TRIPOD-AI) and risk of bias tool (PROBAST-AI) for diagnostic and prognostic prediction model studies based on artificial intelligence. *BMJ Open*. 2021;11(7):e048008. doi:10.1136/bmjopen-2020-048008

SUPPLEMENT 1.

eMethods 1. Searching Strategy and RSS Feed

eMethods 2. Literature Searching Pipeline and Data Extraction/Coding

eMethods 3. Geospatial Model

eMethods 4. PROBAST Assessment Criterion

eMethods 5. CLEAR Modification

eMethods 6. Cohen Kappa Test and Heterogeneity

eTable 1. Modified CLEAR Signaling Questions

eTable 2. Academic Background Distribution for Included Studies

eTable 3. Distribution for Psychiatric Categories in Existing AI Models

eTable 4. Distribution for AI Algorithms in These Models

eTable 5. Distribution for Toolkit of These AI Models

eTable 6. Distribution for Future Selection Methods of These AI Models

eTable 7. Distribution for Cross-Validation Regimes of These AI Models

eTable 8. Distribution for Neuroimaging-based Data Modality of These AI Models

eTable 9. Distribution for Preprocessing Method of These AI Models

eReferences

SUPPLEMENT 2.

Data Sharing Statement